

SLC19A1 transports immunoreactive cyclic dinucleotides

Rutger D. Luteijn^{1,7}, Shivam A. Zaver^{2,7}, Benjamin G. Gowen^{3,4}, Stacia K. Wyman³, Nick E. Garelis¹, Liberty Onia¹, Sarah M. McWhirter⁵, George E. Katibah⁵, Jacob E. Corn^{3,4,6}, Joshua J. Woodward² & David H. Raulet^{1*}

The accumulation of DNA in the cytosol serves as a key immunostimulatory signal associated with infections, cancer and genomic damage^{1,2}. Cytosolic DNA triggers immune responses by activating the cyclic GMP–AMP synthase (cGAS)–stimulator of interferon genes (STING) pathway³. The binding of DNA to cGAS activates its enzymatic activity, leading to the synthesis of a second messenger, cyclic guanosine monophosphate–adenosine monophosphate (2′3′-cGAMP)^{4–7}. This cyclic dinucleotide (CDN) activates STING⁸, which in turn activates the transcription factors interferon regulatory factor 3 (IRF3) and nuclear factor κ -light-chain-enhancer of activated B cells (NF- κ B), promoting the transcription of genes encoding type I interferons and other cytokines and mediators that stimulate a broader immune response. Exogenous 2′3′-cGAMP produced by malignant cells⁹ and other CDNs, including those produced by bacteria^{10–12} and synthetic CDNs used in cancer immunotherapy^{13,14}, must traverse the cell membrane to activate STING in target cells. How these charged CDNs pass through the lipid bilayer is unknown. Here we used a genome-wide CRISPR-interference screen to identify the reduced folate carrier SLC19A1, a folate–organic phosphate antiporter, as the major transporter of CDNs. Depleting SLC19A1 in human cells inhibits CDN uptake and functional responses, and overexpressing SLC19A1 increases both uptake and functional responses. In human cell lines and primary cells ex vivo, CDN uptake is inhibited by folates as well as two medications approved for treatment of inflammatory diseases, sulfasalazine and the antifolate methotrexate. The identification of SLC19A1 as the major transporter of CDNs into cells has implications for the immunotherapeutic treatment of cancer¹³, host responsiveness to CDN-producing pathogenic microorganisms¹¹ and—potentially—for some inflammatory diseases.

To systematically identify genes involved in intracellular transport of CDNs, we performed a genome-wide CRISPR interference (CRISPRi) forward genetic screen in the monocytic THP-1 cell line. To visualize STING activation, THP-1 cells were transduced with a CDN-inducible reporter construct (Fig. 1a, b). Consistent with previous results, the synthetic CDN 2′3′-RR-S2 cyclic di-AMP (2′3′-RR CDA, Extended Data Fig. 1a) induced a more potent response than 2′3′-cGAMP¹³, and the response to both CDNs was severalfold higher than the response to human interferon- β (IFN- β). The response to CDNs was completely dependent on STING expression (Fig. 1b), implying that the reporter primarily reported cell-intrinsic STING activity. For the screen, THP-1 cells expressing a catalytically inactive Cas9 (dCas9) fusion with blue fluorescent protein (BFP) and the transcriptional repression domain KRAB (dCas9–BFP–KRAB), and transduced with a genome-wide guide-RNA (gRNA) library, were stimulated separately with 2′3′-RR CDA or 2′3′-cGAMP, and the highest and lowest quartiles of reporter-expressing cells were sorted by flow cytometry before deep-sequencing to identify gRNAs enriched in each population (Fig. 1c, d, Extended

Data Figs. 1b, 2, Supplementary Tables 1, 2). The two screens yielded many common hits but there were differences, such as numerous hits in the 2′3′-cGAMP screen—including STAT2, IRF9, IFNAR1 and IFNAR2 (Supplementary Table 2). Hence, the 2′3′-RR CDA screen may have mostly been dependent on intrinsic STING signalling, whereas

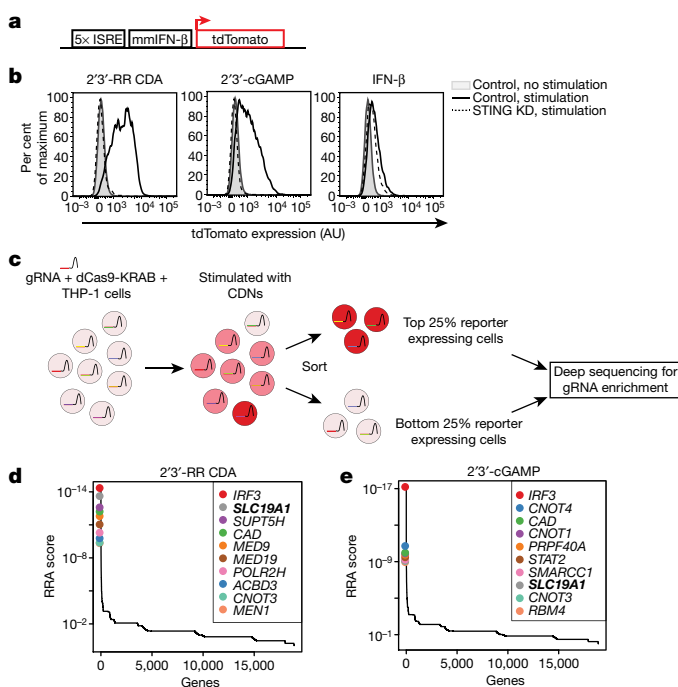


Fig. 1 | Genome-wide CRISPRi screen for host factors necessary for stimulation by CDNs. **a**, Schematic overview of the tdTomato reporter construct. tdTomato expression is driven by interferon-stimulatory response elements (ISRE) followed by a mouse minimal interferon- β (mmiIFN- β) promoter. **b**, Control THP-1 cells and STING-depleted (STING KD) THP-1 cells were incubated with 2′3′-RR CDA (1.67 μ g ml⁻¹), 2′3′-cGAMP (10 μ g ml⁻¹) or human IFN- β (100 ng ml⁻¹). After 20 h, tdTomato reporter expression was analysed by flow cytometry. Data are representative of three independent experiments with similar results. **c**, Schematic overview of the genome-wide CRISPRi screen. A genome-wide library of CRISPRi gRNA-expressing THP-1 cells was stimulated with CDNs. Twenty hours after stimulation, cells were sorted into a tdTomato^{low} group (lowest 25% of cells) and a tdTomato^{high} group (highest 25% of cells). DNA from the sorted cells was deep-sequenced to reveal gRNA enrichment in the two groups. **d**, **e**, Distribution of the robust rank aggregation (RRA) score in the comparison of hits enriched in the tdTomato^{low} versus tdTomato^{high} groups of THP-1 cells stimulated with 2′3′-RR CDA (**d**) or 2′3′-cGAMP (**e**). Each panel represents combined results of two independent screens. AU, arbitrary units.

¹Department of Molecular and Cell Biology, and Cancer Research Laboratory, Division of Immunology and Pathogenesis, University of California, Berkeley, CA, USA. ²Department of Microbiology, University of Washington, Seattle, WA, USA. ³Innovative Genomics Institute, University of California, Berkeley, Berkeley, CA, USA. ⁴Department of Molecular and Cell Biology, University of California, Berkeley, Berkeley, CA, USA. ⁵Aduro Biotech, Berkeley, CA, USA. ⁶Present address: Institute of Molecular Health Sciences, Department of Biology, ETH Zurich, Zurich, Switzerland. ⁷These authors contributed equally: Rutger D. Luteijn, Shivam A. Zaver. *e-mail: raulet@berkeley.edu

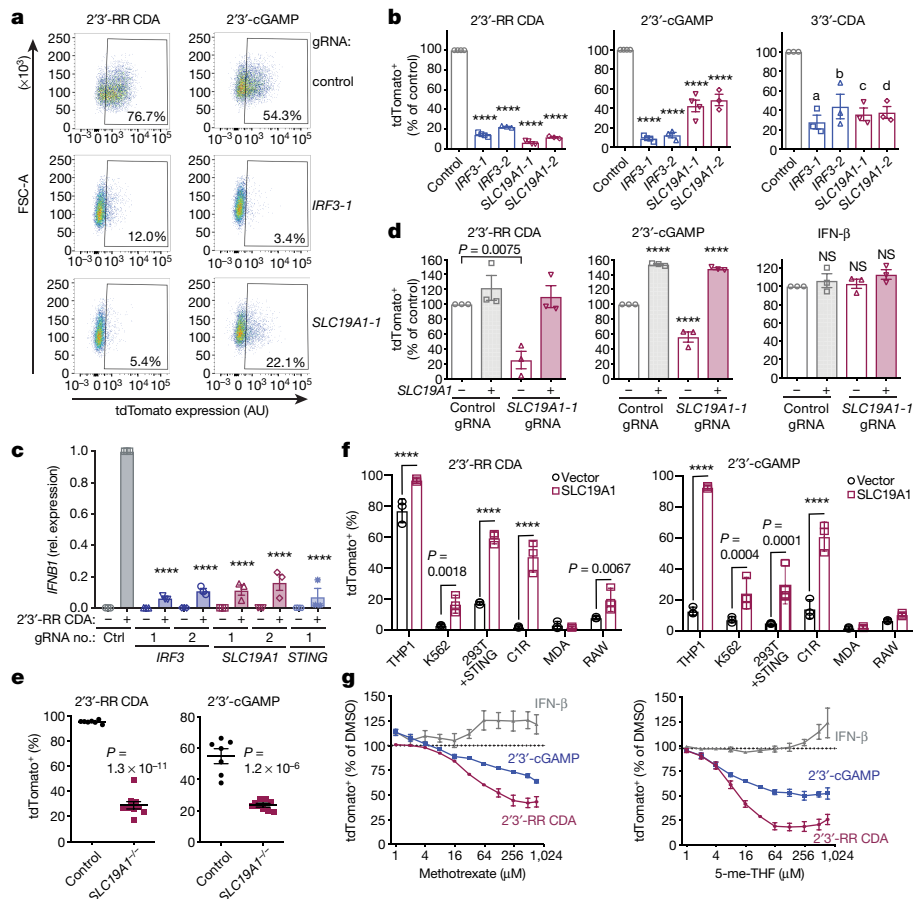


Fig. 2 | SLC19A1 is required for CDN-induced reporter expression.

a, dCas9–KRAB-expressing THP-1 cells transduced with non-targeting gRNA (control), *IRF3-1* gRNA or *SLC19A1-1* gRNA were exposed to 2'3'-RR CDA ($1.67 \mu\text{g ml}^{-1}$) or 2'3'-cGAMP ($15 \mu\text{g ml}^{-1}$). Twenty hours later, tdTomato expression was analysed by flow cytometry. Representative dot plots of three independent experiments are shown. **b**, THP-1 cells expressing the indicated CRISPRi gRNAs or non-targeting gRNA (control), were stimulated with 2'3'-RR CDA ($1.67 \mu\text{g ml}^{-1}$), 2'3'-cGAMP ($10 \mu\text{g ml}^{-1}$), or 3'3'-CDA ($20 \mu\text{g ml}^{-1}$). After 18–22 h, tdTomato expression was quantified as in **a**. **c**, Induction of *IFNβ* mRNA in control (non-targeting gRNA) THP-1 cells or THP-1 cells expressing the indicated CRISPRi gRNAs after 5 h stimulation with $5 \mu\text{g ml}^{-1}$ 2'3'-RR CDA. Rel., relative. **d**, Control THP-1 cells and THP-1 cells expressing *SLC19A1-1* gRNA transduced with *SLC19A1-1* were stimulated with 2'3'-RR CDA ($1.67 \mu\text{g ml}^{-1}$), 2'3'-cGAMP ($15 \mu\text{g ml}^{-1}$) or IFN- β (100 ng ml^{-1}) and analysed as in **a**. **e**, Control THP-1 cells ($n = 7$ independent clonal lines)

and *SLC19A1*^{-/-} cells ($n = 9$ independent clonal lines) were exposed to 2'3'-RR CDA ($2.22 \mu\text{g ml}^{-1}$) or 2'3'-cGAMP ($10 \mu\text{g ml}^{-1}$) and reporter tdTomato expression was analysed as in **a**. Data are mean \pm s.e.m. **f**, Various cell lines expressing a control vector or an *SLC19A1* expression vector were stimulated and analysed as in **a**. **g**, THP-1 cells were incubated with increasing concentrations of the competitive inhibitors methotrexate, 5-me-THF or DMSO as vehicle control, before stimulation with 2'3'-RR CDA ($1.25 \mu\text{g ml}^{-1}$), 2'3'-cGAMP ($15 \mu\text{g ml}^{-1}$) or IFN- β (100 ng ml^{-1}). Cells were analysed as in **a**. For each stimulant, the data were normalized to the DMSO controls. In **b–d**, **f**, **g**, data are mean \pm s.e.m. of $n = 3$ biological replicates. Statistical analyses were performed using one-way analysis of variance (ANOVA) followed by post hoc Dunnett's test for the comparison to stimulated control cells (**b–d**), unpaired two-tailed Student's *t*-tests (**e**) or two-way ANOVA followed by uncorrected Fisher's least significant difference tests (**f**). ^a $P = 0.0002$, ^b $P = 0.0013$, ^c $P = 0.0005$, ^d $P = 0.0006$ and $****P \leq 0.0001$. NS, not significant.

the 2'3'-cGAMP screen may have been partly dependent on autocrine–paracrine IFN- β signalling.

In both screens, the top hits in the hypo-responsive population (that is, the genes that are most important for robust responses to CDNs) included the gene for the transcription factor IRF3, which acts directly downstream of STING. A gRNA for *STING* (also known as *TMEM173*) was also enriched in hypo-responsive cells from both screens, but other *STING* gRNAs were not enriched—presumably because they were ineffective at interfering with *STING* expression (Supplementary Tables 1, 2).

SLC19A1 was one of the most significant hits in both screens. *SLC19A1* is a folate–organic phosphate antiporter that transports folates, structurally similar antifolates and a variety of organic phosphates encompassing (among others) thiamine derivatives and nucleotides^{15,16}. Folate import is coupled to organic phosphate export and many inhibition and exchange phenomena have previously been demonstrated^{17–19}.

To validate the role of *SLC19A1* in CDN stimulation, the top two enriched *SLC19A1*-targeting gRNAs from the 2'3'-RR CDA screen were

used to stably deplete *SLC19A1* in THP-1 cells expressing dCas9–KRAB (Extended Data Fig. 3a). *SLC19A1*-depleted cells grew normally, but uptake of the *SLC19A1* substrate methotrexate was nearly abolished in these cells²⁰ (Extended Data Fig. 3c). Similar to *IRF3*-depleted cells, *SLC19A1*-depleted THP-1 or U937 cells (Extended Data Fig. 3b) were defective in reporter responses induced by 2'3'-cGAMP, 2'3'-RR CDA and 3'3'-CDA (a bacterial CDN that stimulates STING), but responded normally to IFN- β stimulation (Fig. 2a, b, Extended Data Fig. 3d–f). *SLC19A1* depletion—similar to depletion of *IRF3* or *STING*—also inhibited CDN-induced expression of direct downstream target genes in the STING pathway, including *IFNβ* and the chemokine genes *CCL5* and *CXCL10*^{21,22} (Fig. 2c, Extended Data Fig. 3g–i). Transduction of *SLC19A1* into depleted THP-1 cells rescued CDN responsiveness (Fig. 2d). *SLC19A1* disruption using the conventional CRISPR–Cas9 system similarly decreased responsiveness to CDNs in THP-1 cells (Fig. 2e).

SLC19A1 overexpression robustly increased CDN responsiveness in wild-type THP-1 cells and in cell lines that normally respond poorly

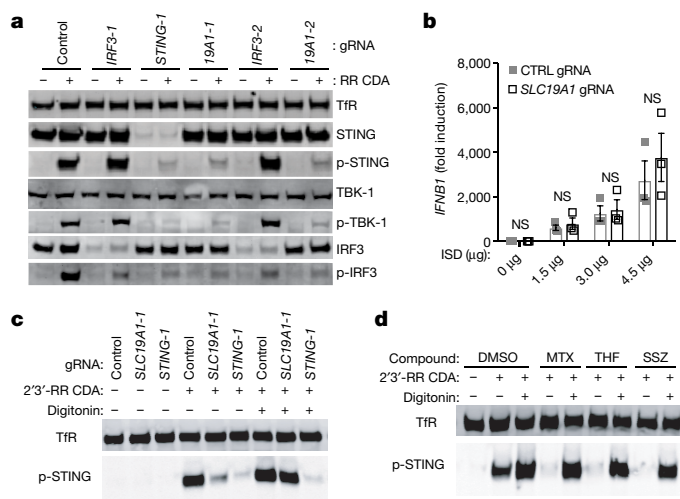


Fig. 3 | SLC19A1 is critical for STING-dependent responses to exogenous CDNs but not when CDNs are provided intracellularly. **a**, Immunoblot analysis of protein expression and phosphorylation in control THP-1 cells or THP-1 cells expressing the indicated CRISPRi gRNAs. Cells were stimulated for 2 h with $10 \mu\text{g ml}^{-1}$ 2'3'-RR CDA (RR CDA) or left unstimulated. p-TBK1, TBK1 phosphorylated on Ser172; p-IRF3, IRF3 phosphorylated on Ser366. **b**, Control (CTRL) THP-1 cells or SLC19A1-depleted THP-1 cells were transfected with increasing amounts of interferon-stimulatory DNA (ISD) for 3 h and induction of *IFNβ1* mRNA was measured by quantitative PCR with reverse transcription (RT-qPCR). **c**, Cells were stimulated as in **a** in the absence or presence of digitonin ($5 \mu\text{g ml}^{-1}$). **d**, Control THP-1 cells were stimulated as in **c**, with the addition of the indicated SLC19A1 inhibitors (all at $750 \mu\text{M}$): methotrexate (MTX), 5-me-THF (THF), sulfasalazine (SSZ) or DMSO (as vehicle control). Tfr, transferrin receptor. Data in **a**, **c**, and **d** are representative of $n = 3$ biological replicates. For gel source data, see Supplementary Fig. 1. In **b**, data are mean \pm s.e.m. of $n = 3$ biological replicates and statistical analyses were performed using two-way ANOVA followed by post hoc Sidak's test.

(or not at all) to CDN stimulation, including C1R, K562 and 293T cells (pre-transduced with STING) (Fig. 2f, Extended Data Figs. 3j, 4). Together, our data show reduced CDN responses in *SLC19A1*-deficient cells and amplified responses in cells that overexpress *SLC19A1*.

Inhibitor experiments showed that the known *SLC19A1* substrates methotrexate and 5-methyl-tetrahydrofolic acid (5-me-THF)¹⁵ blocked stimulation of THP-1 cells by 2'3'-cGAMP or 2'3'-RR CDA at concentrations only modestly higher than those that inhibit uptake of folate derivatives²³, but did not inhibit reporter responses to IFN- β (Fig. 2g). At high concentrations, the non-competitive *SLC19A1* inhibitor sulfasalazine²³ blocked responses to CDNs and to IFN- β stimulation, which suggests a broader effect on reporter activation (Extended Data Fig. 3k).

To directly assess the effect of *SLC19A1* on STING pathway activation (Extended Data Fig. 5a), we used immunoblotting to evaluate phosphorylation of STING, IRF3 and TBK1 induced by a 2-h exposure to 2'3'-RR CDA in control (non-targeting gRNA) versus CRISPRi-depleted cells (Fig. 3a). As expected, *STING* depletion inhibited phosphorylation of both TBK1 and IRF3, whereas *IRF3* depletion did not inhibit phosphorylation of TBK1 or STING. By contrast, *SLC19A1* depletion resulted in major defects in phosphorylation of STING, TBK1 and IRF3, which indicates that *SLC19A1* acts upstream of STING.

Protein levels of STING, TBK1 and IRF3 were unaltered in *SLC19A1*-depleted cells. Notably, *SLC19A1*-depleted cells responded normally when transfected with DNA (Fig. 3b). Furthermore, when transport was bypassed by permeabilizing *SLC19A1*-depleted cells with digitonin, STING exhibited a normal phosphorylation response to CDNs (Fig. 3c). Similarly, the inhibitory effects on CDN-induced STING phosphorylation and gene expression of *SLC19A1* blockers—including

methotrexate, 5-me-THF and the irreversible, covalent *SLC19A1* inhibitor *N*-hydroxysuccinimide (NHS)-methotrexate (Methods)—were bypassed when the cells were permeabilized with digitonin (Fig. 3d, Extended Data Fig. 5b–f). Thus, STING functioned normally in *SLC19A1*-depleted or inhibited cells when CDNs or DNA were introduced directly into the cytosol, consistent with a role for *SLC19A1* in CDN transport.

To directly test the effect of *SLC19A1* on transport, we monitored cellular uptake of ^{32}P -labelled CDNs (Extended Data Fig. 6a–h). *SLC19A1* overexpression resulted in a two- to three-fold enhancement of [^{32}P]2'3'-cGAMP uptake by THP-1, K562 and C1R cells (Fig. 4a, b, Extended Data Fig. 6i). Conversely, *SLC19A1* depletion reduced the uptake of [^{32}P]2'3'-cGAMP in THP-1 and K562 cells (Fig. 4a, b, Extended Data Fig. 6j–m). Furthermore, we observed reduced 2'3'-cGAMP influx in THP-1 and K562 cells treated with NHS-methotrexate (Fig. 4c). Uptake of 2'3'-cGAMP by THP-1 cells was also inhibited by excess unlabelled 2'3'-cGAMP as well as by the bacterial CDNs 3'3'-cGAMP, 3'3'-CDA and 3'3' c-di-GMP. Thus, CDN interactions with the transporter are not highly specific for the 2'3' linkage or the specific nucleotides (Fig. 4d). The nucleoside monophosphates AMP and GMP—the major ENPP1 hydrolysis products of 2'3'-cGAMP—slightly inhibited uptake of [^{32}P]2'3'-cGAMP²⁴ (Fig. 4d), consistent with previous observations that AMP, other nucleotides and organic phosphates in general inhibit *SLC19A1*-mediated transport^{17,18}. Our findings indicate that *SLC19A1* broadly interacts with CDNs irrespective of the phosphodiester linkages or the base content, but that breakdown products of CDNs have a limited effect on CDN uptake.

Sustained inhibition of 2'3'-cGAMP uptake occurred when folic acid, 5-me-THF, methotrexate or sulfasalazine were added to the culture medium of various cell lines (Fig. 4e, Extended Data Fig. 6n–o). In terms of half-maximum inhibitory concentration (IC_{50}), sulfasalazine ($\text{IC}_{50} = 2.1 \mu\text{M}$) and folic acid ($\text{IC}_{50} = 4.8 \mu\text{M}$) were in the same range as 2'3'-cGAMP ($\text{IC}_{50} = 1.89 \mu\text{M}$) (Extended Data Fig. 6p), similar to the dosage of 2'3'-cGAMP required for STING activation and interferon responses ($10\text{--}20 \mu\text{M}$) (Extended Data Fig. 3d). Consistent with their much higher affinity for *SLC19A1* binding compared with folic acid, 5-me-THF ($\text{IC}_{50} = 4.1 \text{ nM}$) and methotrexate ($\text{IC}_{50} = 54.8 \text{ nM}$) were much more potent inhibitors of CDN uptake¹⁷ (Extended Data Fig. 6p). Notably, 5-me-THF incompletely inhibited [^{32}P]2'3'-cGAMP uptake, unlike the other folates or antifolates. Consistent with an antiporter mechanism of uptake, preloading the cells with 5-me-THF—which *trans*-stimulates *SLC19A1* import²⁵—augmented 2'3'-cGAMP influx (Extended Data Fig. 6q). These observations establish that CDN import is altered by known substrates and inhibitors of the *SLC19A1* transporter in a wide range of human cell lines.

We next monitored 2'3'-cGAMP uptake in primary healthy adult human peripheral blood mononuclear cells (PBMCs). Treatment of PBMCs with NHS-methotrexate, or excess, unlabelled 5-me-THF, methotrexate or sulfasalazine strongly inhibited [^{32}P]2'3'-cGAMP uptake (Fig. 4f, Extended Data Fig. 6r). These data generalize our findings to normal human blood cells.

In contrast to these results in human cells, neither CDN uptake nor CDN-induced *Cxcl10* expression was inhibited by depleting *Slc19a1* expression in the mouse C1498 or L1210 cell lines, the latter of which has extensively been studied in the context of *SLC19A1*-mediated transport^{17,18,26} (Extended Data Fig. 7). *Slc19a1* depletion in mouse bone-marrow-derived macrophages or dendritic cells also did not block *Ifn* gene expression induced by CDNs (Extended Data Fig. 7i–l). Furthermore, antifolates that inhibit *SLC19A1*, including methotrexate, did not inhibit 2'3'-cGAMP uptake by mouse splenocytes (Extended Data Fig. 7m–o). Collectively, these results suggested that *SLC19A1* expression and function are essential for uptake of the metazoan CDN 2'3'-cGAMP by human cell lines and human primary cells *ex vivo*, but not by the mouse cells we studied. Therefore, mouse cells probably express another potent CDN transporter.

SLC19A1-mediated import of CDNs would require a direct interaction with the CDN. Consistent with this hypothesis, His-tagged

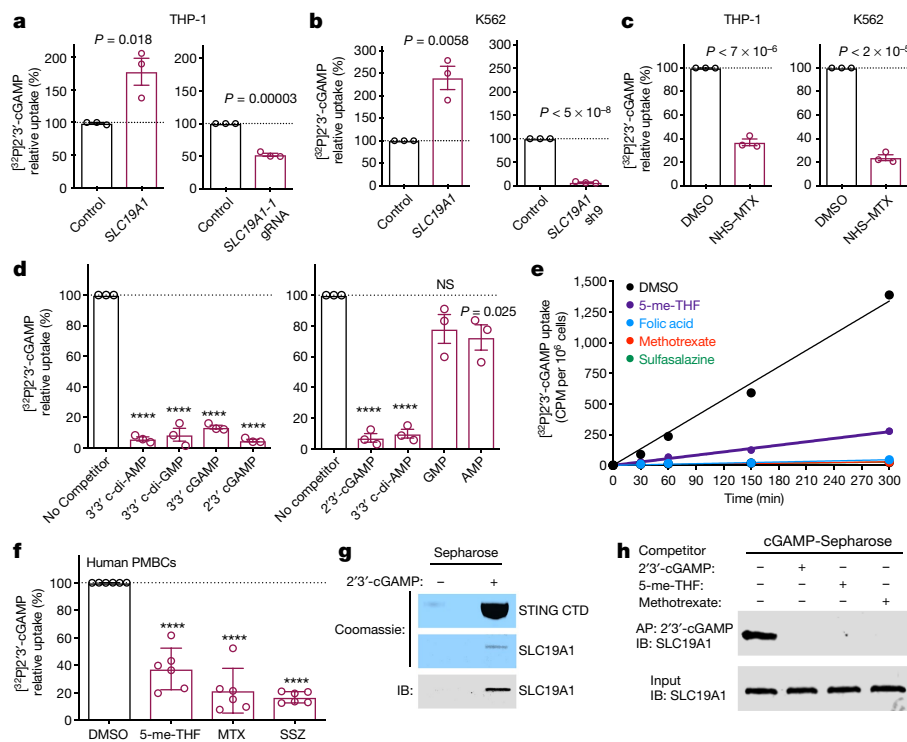


Fig. 4 | SLC19A1 transports CDNs. **a**, Normalized [32 P]2′3′-cGAMP uptake after 1 h by THP-1 monocytes transduced with empty vector (control) or *SLC19A1* expression vector (left) or with a non-targeting control CRISPRi gRNA or *SLC19A1* CRISPRi gRNA (right). **b**, Normalized [32 P]2′3′-cGAMP uptake after 1 h by K562 cells transduced with empty vector (control) or *SLC19A1* expression vector (left) or with a non-targeting control shRNA (control) or *SLC19A1* shRNA (right). **c**, Normalized [32 P]2′3′-cGAMP uptake in THP-1 (left) and K562 (right) cells after 1 h in DMSO or NHS-methotrexate (NHS-MTX, 5 μ M)-treated. **d**, Normalized [32 P]2′3′-cGAMP uptake after 1 h by THP-1 monocytes in the presence and absence of 100 μ M competing, unlabelled CDNs (left) or 200 μ M competing, unlabelled nucleotides (right). **e**, Time course of [32 P]2′3′-cGAMP uptake in THP-1 monocytes in the presence and absence of 500 μ M competing, unlabelled folates, antifolates or sulfasalazine. CPM, counts per minute. **f**, Normalized [32 P]2′3′-cGAMP

uptake after 3 h in human PBMCs from 6 healthy donors in the presence or absence of 500 μ M competing, unlabelled folates, antifolates or sulfasalazine. **g**, Coomassie staining and immunoblot (IB) analysis of pull-downs by 2′3′-cGAMP-Sepharose or control Sepharose of STING C-terminal domain (CTD) or hSLC19A1. **h**, Western blot analysis of hSLC19A1 affinity purification (AP) with 2′3′-cGAMP-Sepharose in the absence or presence of free, unbound 2′3′-cGAMP, 5-me-THF or methotrexate (250 μ M). In **a–d**, data are mean \pm s.e.m. of $n = 3$ biological replicates. In **e**, data are mean \pm s.d. of $n = 3$ technical replicates and representative of 3 independent experiments. In **f**, data are mean \pm s.d. of $n = 6$ healthy donors over 2 independent experiments. **g** and **h** are representative of two independent experiments; for gel source data, see Supplementary Fig. 1. Statistical analyses were performed using unpaired, two-tailed Student's *t*-tests (**a–d**), or one-way ANOVA followed by post hoc Tukey's test (**f**). **** $P \leq 0.0001$.

SLC19A1 was precipitated by 2′3′-cGAMP immobilized on Sepharose beads (Fig. 4g, Extended Data Fig. 8a, b). This interaction was competitively disrupted by free, unbound 2′3′-cGAMP and 3′3′-CDA (Fig. 4h, Extended Data Fig. 8c) or by 5-me-THF and methotrexate (Fig. 4h). These data suggest that CDNs interact with SLC19A1, consistent with its proposed role as a CDN transporter. Taken together, our results demonstrate that SLC19A1 is a CDN transporter in human cells, which is required for activation of type I interferon mediated by exogenous CDNs.

The response to CDNs was relatively weak in most cell lines that we tested and was increased by overexpression of *SLC19A1* or permeabilization of cells (Figs. 2f, 3c). Among a large set of cell lines, THP-1 cells are among the highest in expression of both *SLC19A1* and *STING* (Extended Data Fig. 9). It is likely that expression of *SLC19A1* and *STING* are each important predictors of the responsiveness of cell lines and tumours to CDN stimulation.

Methotrexate, folic acid and sulfasalazine almost completely blocked CDN uptake and/or stimulation, whereas CDN stimulation was not completely inhibited in *SLC19A1*-null cells. This implies that another transporter sensitive to these drugs may have a role in CDN uptake. Although it was not a hit in our screen, overexpression of *SLC46A1*, which encodes the only other known folate transporter¹⁵, increased responses to CDNs (Extended Data Fig. 10a). However, depletion of *SLC46A1* (approximately 90% reduction in mRNA) had little or no effect on CDN stimulation, even when combined with depletion of

SLC19A1 (Extended Data Fig. 10c). Overexpression of *SLC46A3*, another hit in our screen, increased the response to CDNs (Extended Data Fig. 10b) and depletion of *SLC46A3* (90% effective) had a minor effect on reporter induction by both CDNs (Extended Data Fig. 10d). However, depleting both *SLC19A1* and *SLC46A3* together did not reduce responses more than depletion of *SLC19A1* alone (Extended Data Fig. 10d), which suggests that neither *SLC46A3* nor *SLC46A1* is responsible for most of the residual CDN transport in *SLC19A1*-depleted cells.

Our findings extend the spectrum of organic phosphates that use SLC19A1 to 2′3′-cGAMP, 2′3′-RR CDA and probably other CDNs, by the direct measurement of their transport and the effect of extracellular and intracellular folates on their uptake in human cells by this route. In this context, SLC19A1 could have an important role in the antitumour and adjuvant effects of CDNs administered to patients. It may also be important in cell-to-cell transport of CDNs in immune responses or immune pathology. For example, the SLC19A1 inhibitors methotrexate and sulfasalazine are first-line treatments in rheumatoid arthritis and are widely used to treat inflammatory bowel diseases, including ulcerative colitis and Crohn's disease^{27–29}. Although no direct evidence for this is available in humans, studies in mouse models of inflammatory bowel disease raise the possibility that host cells import CDNs produced by intestinal bacteria, activating STING in a cGAS-independent fashion³⁰. It remains to be determined whether SLC19A1 has a role in such processes in humans. In conclusion, we have identified

SLC19A1—in humans—as a CDN transporter with potential relevance in the context of cancer immunotherapy and immunopathology.

Online content

Any methods, additional references, Nature Research reporting summaries, source data, extended data, supplementary information, acknowledgements, peer review information; details of author contributions and competing interests; and statements of data and code availability are available at <https://doi.org/10.1038/s41586-019-1553-0>.

Received: 21 November 2018; Accepted: 8 August 2019;

Published online 11 September 2019.

- Ishii, K. J. et al. A Toll-like receptor-independent antiviral response induced by double-stranded B-form DNA. *Nat. Immunol.* **7**, 40–48 (2006).
- Stetson, D. B. & Medzhitov, R. Recognition of cytosolic DNA activates an IRF3-dependent innate immune response. *Immunity* **24**, 93–103 (2006).
- Li, T. & Chen, Z. J. The cGAS–cGAMP–STING pathway connects DNA damage to inflammation, senescence, and cancer. *J. Exp. Med.* **215**, 1287–1299 (2018).
- Sun, L., Wu, J., Du, F., Chen, X. & Chen, Z. J. Cyclic GMP–AMP synthase is a cytosolic DNA sensor that activates the type I interferon pathway. *Science* **339**, 786–791 (2013).
- Gao, P. et al. Cyclic [G(2',5')pA(3',5')p] is the metazoan second messenger produced by DNA-activated cyclic GMP–AMP synthase. *Cell* **153**, 1094–1107 (2013).
- Ablasser, A. et al. cGAS produces a 2'-5'-linked cyclic dinucleotide second messenger that activates STING. *Nature* **498**, 380–384 (2013).
- Diner, E. J. et al. The innate immune DNA sensor cGAS produces a noncanonical cyclic dinucleotide that activates human STING. *Cell Rep.* **3**, 1355–1361 (2013).
- Ishikawa, H. & Barber, G. N. STING is an endoplasmic reticulum adaptor that facilitates innate immune signalling. *Nature* **455**, 674–678 (2008).
- Marcus, A. et al. Tumor-derived cGAMP triggers a STING-mediated interferon response in non-tumor cells to activate the NK cell response. *Immunity* **49**, 754–763 (2018).
- Woodward, J. J., Iavarone, A. T. & Portnoy, D. A. c-di-AMP secreted by intracellular *Listeria monocytogenes* activates a host type I interferon response. *Science* **328**, 1703–1705 (2010).
- McWhirter, S. M. et al. A host type I interferon response is induced by cytosolic sensing of the bacterial second messenger cyclic-di-GMP. *J. Exp. Med.* **206**, 1899–1911 (2009).
- Burdette, D. L. et al. STING is a direct innate immune sensor of cyclic di-GMP. *Nature* **478**, 515–518 (2011).
- Corrales, L. et al. Direct activation of STING in the tumor microenvironment leads to potent and systemic tumor regression and immunity. *Cell Rep.* **11**, 1018–1030 (2015).
- Corrales, L., McWhirter, S. M., Dubensky, T. W., Jr & Gajewski, T. F. The host STING pathway at the interface of cancer and immunity. *J. Clin. Invest.* **126**, 2404–2411 (2016).
- Hou, Z. & Matherly, L. H. Biology of the major facilitative folate transporters SLC19A1 and SLC46A1. *Curr. Top. Membr.* **73**, 175–204 (2014).
- Zhao, R., Diop-Bove, N., Visentin, M. & Goldman, I. D. Mechanisms of membrane transport of folates into cells and across epithelia. *Annu. Rev. Nutr.* **31**, 177–201 (2011).
- Henderson, G. B. & Zevely, E. M. Structural requirements for anion substrates of the methotrexate transport system in L1210 cells. *Arch. Biochem. Biophys.* **221**, 438–446 (1983).
- Goldman, I. D. The characteristics of the membrane transport of amethopterin and the naturally occurring folates. *Ann. NY Acad. Sci.* **186**, 400–422 (1971).
- Yang, C. H., Sirotnak, F. M. & Dembo, M. Interaction between anions and the reduced folate/methotrexate transport system in L1210 cell plasma membrane vesicles: directional symmetry and anion specificity for differential mobility of loaded and unloaded carrier. *J. Membr. Biol.* **79**, 285–292 (1984).
- Goldman, I. D., Lichtenstein, N. S. & Oliverio, V. T. Carrier-mediated transport of the folic acid analogue, methotrexate, in the L1210 leukemia cell. *J. Biol. Chem.* **243**, 5007–5017 (1968).
- Lin, R., Heylbroeck, C., Genin, P., Pitha, P. M. & Hiscott, J. Essential role of interferon regulatory factor 3 in direct activation of RANTES chemokine transcription. *Mol. Cell. Biol.* **19**, 959–966 (1999).
- Brownell, J. et al. Direct, interferon-independent activation of the CXCL10 promoter by NF- κ B and interferon regulatory factor 3 during hepatitis C virus infection. *J. Virol.* **88**, 1582–1590 (2014).
- Jansen, G. et al. Sulfasalazine is a potent inhibitor of the reduced folate carrier: implications for combination therapies with methotrexate in rheumatoid arthritis. *Arthritis Rheum.* **50**, 2130–2139 (2004).
- Kato, K. et al. Structural insights into cGAMP degradation by ecto-nucleotide pyrophosphatase phosphodiesterase 1. *Nat. Commun.* **9**, 4424 (2018).
- Goldman, I. D. A model system for the study of heteroexchange diffusion: methotrexate–folate interactions in L1210 leukemia and Ehrlich ascites tumor cells. *Biochim. Biophys. Acta* **233**, 624–634 (1971).
- Henderson, G. B., Grzelakowska-Sztabert, B., Zevely, E. M. & Huennekens, F. M. Binding properties of the 5-methyltetrahydrofolate/methotrexate transport system in L1210 cells. *Arch. Biochem. Biophys.* **202**, 144–149 (1980).
- Plosker, G. L. & Croom, K. F. Sulfasalazine: a review of its use in the management of rheumatoid arthritis. *Drugs* **65**, 1825–1849 (2005).
- Kozuch, P. L. & Hanauer, S. B. Treatment of inflammatory bowel disease: a review of medical therapy. *World J. Gastroenterol.* **14**, 354–377 (2008).
- Rajitha, P., Biswas, R., Sabitha, M. & Jayakumar, R. Methotrexate in the treatment of psoriasis and rheumatoid arthritis: mechanistic insights, current issues and novel delivery approaches. *Curr. Pharm. Des.* **23**, 3550–3566 (2017).
- Ahn, J., Son, S., Oliveira, S. C. & Barber, G. N. STING-dependent signaling underlies IL-10 controlled inflammatory colitis. *Cell Rep.* **21**, 3873–3884 (2017).

Publisher's note Springer Nature remains neutral with regard to jurisdictional claims in published maps and institutional affiliations.

© The Author(s), under exclusive licence to Springer Nature Limited 2019

METHODS

No statistical methods were used to predetermine sample size. The experiments were not randomized. The investigators were not blinded to allocation during experiments and outcome assessment.

Cell culture. All cell lines were cultured at 37 °C in humidified atmosphere containing 5% CO₂ with medium supplemented with 100 U ml⁻¹ penicillin, 100 µg ml⁻¹ streptomycin, 0.2 mg ml⁻¹ glutamine, 10 µg ml⁻¹ gentamycin sulfate, 20 mM HEPES and 10% FCS. THP-1, C1R, and K562 cells were cultured in RPMI medium, and 293T, 293T transfected with human STING (293T+hSTING), MDA-MBA-453 (MDA) and RAW 264.7 macrophages were cultured in DMEM medium. Human embryonic kidney 293F cells (HEK293F) were grown in FreeStyle 293 medium supplemented with GlutaMax (GIBCO) at 37 °C in the presence of 5% CO₂ in a shaking incubator. THP-1, K562, 293T cells, and RAW 264.7 macrophages were from existing stocks in the laboratory. MDA-MB-231 cells were obtained from the Berkeley Cell Culture Facility. C1R cells were a gift from V. Spies (Fred Hutchinson Cancer Center). HEK293F cells were a gift from D. Veessler (University of Washington). The 293T+hSTING cells were generated as previously described¹². L1210 cells were obtained from ATCC (CCL-219) and cultured in DMEM including 10% horse serum (Gibco, cat. no. 26-050-088). L1210 cells were authenticated by ATCC. MDA-MBA-453 were authenticated by the Berkeley Cell Culture Facility using karyotyping and/or PCR; other cell lines were not authenticated. All cell lines were negative for mycoplasma contamination.

Antibodies and reagents. The following antibodies were obtained from Cell Signaling Technology: rabbit-anti-human TBK1 monoclonal (clone D1B4; 1:500 for immunoblot), rabbit-anti-human p-TBK1 monoclonal (clone D52C2; 1:1,000 for immunoblot), rabbit-anti-human STING monoclonal (clone D2P2F; 1:2,000 for immunoblot), rabbit-anti-human p-STING monoclonal (clone D7C3S; 1:1,000 for immunoblot), rabbit-anti-human p-IRF3 monoclonal (clone 4D4G; 1:1,000 for immunoblot). Antibodies obtained from LI-COR Biosciences: goat-anti-mouse IgG IRDye 680RD conjugated (cat. no. 926-68070; used at 1:5,000), donkey-anti-rabbit IgG IRDye 800CW conjugated (cat. no. 926-32213; used at 1:5,000), donkey-anti-rabbit IgG IRDye 680RD (cat. no. 926-68073; used at 1:5,000). Other antibodies: rabbit-anti-human IRF3 monoclonal (Abcam, cat. no. EP2419Y; 1:2,000 for immunoblot), mouse-anti-human transferrin receptor monoclonal (Thermo Fisher Scientific, clone H68.4; 1:1,000 for immunoblot), rabbit-anti-human SLC19A1 polyclonal (BosterBio, cat. no. PB9504; 0.4 µg ml⁻¹ for immunoblot), APC-conjugated mouse-anti-human CD55 monoclonal (BioLegend, clone JS11; 1:50 for flow cytometry), mouse-anti-human CD59 monoclonal (BioLegend clone p282; 1:250 for flow cytometry), APC-conjugated goat-anti-mouse IgG (BioLegend, cat. no. 405308; 1:100 for flow cytometry). Reagents used: 5-methyl THF (Cayman Chemical, cat. no. 16159), methotrexate (Cayman Chemical, cat. no. 13960), folic acid (Cayman Chemical, cat. no. 20515), sulfasalazine (Sigma-Aldrich, cat. no. S0883), polybrene (EMD Millipore, cat. no. TR1003G), 3′/3′-cyclic-di-AMP (3′/3′ CDA) (Invivogen, cat. no. tlr-nacda), 2′/3′-RR c-di-AMP (2′/3′-RR-S2 CDA) and 2′/3′-cyclic-di-GMP-AMP (2′/3′-cGAMP) (gifts from Aduro Biotech), human IFN-β (PeproTech, cat. no. 300-02B), mouse IFN-β1 (BioLegend, cat. no. 581302). Antibiotic selection: puromycin (Sigma-Aldrich, cat. no. P8833), blasticidin (Invivogen, cat. no. ant-bl-1; used at 10 µg ml⁻¹), zeocin (Invivogen, cat. no. ant-zn-1; used at 200 µg ml⁻¹).

Plasmids. A gBLOCK gene fragment (Integrated DNA Technologies) encoding the tdTomato reporter gene driven by the ISREs and the minimal mouse IFN-β promoter was cloned into a dual-promoter lentiviral plasmid using Gibson assembly. This lentiviral plasmid co-expressed the zeocin resistance gene and GFP via a T2A ribosomal-skipping sequence controlled by the human EF1A promoter, and was generated as previously described³¹.

For rescue and overexpression of the folate-organic phosphate antiporter *SLC19A1*^{15,26,32–35}, the proton-coupled folate transporter *SLC46A1*¹⁵ or the maytansine transporter *SLC46A3*³⁶, a gBLOCK gene fragment encoding *SLC19A1* (gene ID 6573, transcript 1), *SLC46A1* (gene ID 113235) or *SLC46A3* (gene ID 283537) was cloned by Gibson assembly into a dual-promoter lentiviral plasmid co-expressing the blasticidin resistance gene and the fluorescent gene mAmetrine.

For CRISPRi-mediated depletions, cells were transduced with a lentiviral dCas9-HA-BFP-KRAB-NLS expression vector (Addgene plasmid no. 102244).

For screen validation using individual gRNAs, gRNAs (Supplementary Table 3) were cloned into the same expression plasmid used for the gRNA library (pCRISPRi-v2, Addgene plasmid no. 84832, a gift from J. Weissman). The lentiviral gRNA plasmid co-expressed a puromycin resistance gene and blue fluorescence protein (BFP) via a T2A ribosomal skipping sequence controlled by the human EF1A promoter. The CRISPRi gRNAs introduced into this vector by Gibson assembly were expressed from a mouse U6 promoter. For expression of multiple gRNAs, additional gRNAs were introduced in a separate vector that co-expressed the blasticidin resistance gene and mAmetrine via a T2A ribosomal skipping sequence under the control of a human EF1A promoter.

Conventional CRISPR gRNAs (see Supplementary Table 3) were cloned into a selectable lentiviral CRISPR-Cas9 vector. This lentiviral vector included a human

codon-optimized *Streptococcus pyogenes* Cas9 co-expressing the puromycin resistance gene via a T2A ribosome-skipping sequence under the control of a minimal human EF1A promoter^{31,37}.

Lentiviral production and transduction. Lentivirus was produced by transfecting lentiviral plasmids and second-generation packaging and polymerase plasmids into 293T cells using TransIT-LT1 Reagent (Mirus Bio). Virus-containing supernatants were collected 72 h later, centrifuged to remove cell debris and filtered using a 0.45-µm polyethersulfone filter. Filtered virus supernatant was used to transduce target cells by spin-infection (800g for 90 min at 33 °C) in the presence of 8 µg ml polybrene. After spin infection, virus and polybrene-containing medium was diluted 1:1 with fresh medium. Seventy-two hours after transduction, cells were sorted on the basis of fluorescence expression using a BD FACSAria cell sorter, or selected with the relevant selection reagent for at least seven days.

2′/3′-RR CDA and 2′/3′-cGAMP screens. THP-1 cells co-expressing the tdTomato reporter, GFP and dCas9-BFP were single-cell-sorted to select for a THP-1 cell clone with efficient dCas9-BFP-knockdown capacity. Clones were transduced with lentiviral vectors encoding gRNAs targeting GFP, *CD55* or *CD59*. After one week with puromycin (2 µg ml⁻¹) selection, *CD55*, *CD59* and GFP expression were quantified using the BD LSR Fortessa flow cytometer. A clone that showed the highest reduction in all three marker genes was selected for the screens.

Two separate cultures of THP-1 cells were transduced with the human genome-wide CRISPRi v2 library³⁸. Each culture was divided in two and screened separately after treatment with 2′/3′-RR CDA or 2′/3′-cGAMP, followed by selection and analysis. Hence, each screen was performed twice, with independent library transductions. For each transduction, the THP-1 clone was expanded to 3.2 × 10⁸ cells and transduced with the human genome-wide CRISPRi v2 library³⁸, which contains approximately 100,000 gRNAs targeting around 20,000 genes. Sufficient cells were transduced and propagated to maintain at least 5 × 10⁷ transduced (BFP⁺) cells, representing 500× coverage of the gRNA library. The transduction efficiency was around 20% to minimize the chance of multiple lentiviral integrations per cell. Two days after transduction, cells were cultured in the presence of puromycin for two days and for one additional day without puromycin. Cells (4 × 10⁸) were seeded to a density of 10⁶ cells per ml and stimulated with 2′/3′-RR CDA (2 µg ml⁻¹) or 2′/3′-cGAMP (15 µg ml⁻¹). Twenty hours later, cells were collected, washed in PBS and sorted on the basis of BFP expression (presence of gRNAs), GFP expression (presence of reporter) and tdTomato expression using the BD Influx cell sorter and BD FACSAria Fusion cell sorter. The cells were sorted into two populations on the basis of tdTomato expression: the highest 25% of tdTomato expressing cells (hyper-responsive population) and lowest 25% of tdTomato expressing cells (hypo-responsive population). During sorting, all cells were kept at 4 °C. After sorting, cells were counted: the sorted populations contained 1.5–2 × 10⁷ cells, and the unsorted control contained 1–1.5 × 10⁸ cells. Cells were washed in PBS and cell pellets were stored at –80 °C until further processing.

gDNA isolation and sequencing. Genomic DNA was isolated from sorted cells using NucleoSpin Blood kits (Macherey-Nagel). PCR was used to amplify gRNA cassettes with Illumina sequencing adapters and indexes as previously described³⁹. Genomic DNA samples were first digested for 18 h with *SbfI*-HF (NEB) to liberate a ~500-bp fragment containing the gRNA cassette. The gRNA cassette was isolated by gel electrophoresis as previously described³⁹ using NucleoSpin Gel and PCR Clean-up kits (Macherey-Nagel), and the DNA was then used for PCR. Custom PCR primers are listed in Supplementary Table 5. Indexed samples were pooled and sequenced on an Illumina HiSeq-2500 for the 2′/3′-RR CDA screen and an Illumina HiSeq-4000 for the 2′/3′-cGAMP screen using a 1:1 mix of 2 custom sequencing primers (Supplementary Table 5). Sequencing libraries were pooled proportional to the number of sorted cells in each sample. The target sequencing depth was at least 2,000 reads per gRNA in the library for unsorted ‘background’ samples, and at least 10 reads per cell in sorted samples.

Screen data analysis. CRISPRi samples were analysed using the Python-based ScreenProcessing pipeline (<https://github.com/mhorlbeck/ScreenProcessing>). Normalization using a set of negative control genes and calculations of phenotypes and Mann–Whitney *P* values were performed as previously described^{38,40}. In brief, Illumina 50-bp single-end sequencing reads for pooled sublibraries 1 to 4 and 5 to 7 were trimmed to 29 bp and guides were quantified by counting exact matches to the CRISPRi v.2 human library guides. Phenotypes were calculated as the log₂ fold change in enrichment of an sgRNA in the high and low samples versus background as well as high versus low, normalized by median subtracting non-targeting sgRNAs^{40,41}. Phenotypes from sgRNAs targeting the same gene were collapsed into a single-sensitivity phenotype for each gene using the average of the top three scoring sgRNAs (by phenotype absolute value). For genes with multiple independent transcription start sites (TSSs) targeted by the sgRNA libraries, phenotypes and *P* values were calculated independently for each TSS and then collapsed to a single score by selecting the TSS with the lowest Mann–Whitney *P* value. Counts from the ScreenProcessing pipeline were then used as input to the MAGeCK program to obtain FDR scores for filtering (see Supplementary

Table 2). We integrated multiple gRNAs per gene comparing the hypo-responsive and hyper-responsive populations calculated as RRA scores as depicted in Fig. 1d, e. Similar results were obtained when each sorted population was compared to unsorted cells (Supplementary Table 2).

Genes were also ranked by individual gRNAs with the greatest enrichment or depletion between the hypo-responsive and hyper-responsive libraries. gRNA read counts were normalized to library sequencing depth by converting to read counts per million total reads. For each gRNA, the ratio between the read counts for the hypo-responsive and hyper-responsive libraries was determined and averaged between replicates. For hypo-responsive gene rankings, each gene was ranked by the single corresponding gRNA with the highest hypo-to-hyper ratio (Supplementary Table 1, 'highest ratio hypo/hyper' column). For hyper-responsive gene rankings, each gene was ranked by the single corresponding gRNA with the lowest hypo-to-hyper ratio (Supplementary Table 1, 'lowest ratio hypo/hyper' column). Gene-level phenotypes are available in Supplementary Tables 1, 2.

CDN and IFN- β stimulation assays. The week before stimulation experiments, cells were cultured at the same density. The day before stimulation, cells were seeded to 0.5×10^6 cells per ml. Cells were stimulated with CDNs or IFN- β in 48-well plates using 50,000 cells per well in 300 μ l medium. After 18–24 h, cells were transferred to a 96-well plate and tdTomato expression was measured by flow cytometry using a high-throughput plate reader on a BD LSR Fortessa. For stimulations in the presence of sulfasalazine, 5-me-THF or methotrexate, cells were stimulated in 48-well plates using 20,000 cells per well in 300 μ l medium. Cells were incubated with compounds or DMSO as vehicle before stimulations with CDNs or IFN- β . 18–24h after stimulation, tdTomato reporter expression was quantified by flow cytometry using a high-throughput plate reader on a BD LSR Fortessa.

Production of *SLC19A1*-knockout cell lines. As an alternative approach to corroborate the role of *SLC19A1* in CDN responses, *SLC19A1* was disrupted in THP-1 cells using the conventional CRISPR-Cas9 system. THP-1 cells expressing the tdTomato reporter were transduced with a CRISPR-Cas9 lentiviral plasmid encoding a control gRNA or a gRNA targeting *SLC19A1* at a region critical for transport⁴² (Supplementary Table 3). Transduced cells were selected using puromycin for two days and single-cell-sorted using a BD FACSAria cell sorter. Control cells and *SLC19A1*-targeted cells were selected that had comparable forward and side scatter by flow cytometry analysis. Genomic DNA was isolated from clones using the Qiamp DNA minikit (Qiagen), and the genomic region surrounding the *SLC19A1* gRNA target site was amplified by PCR using primers 5'-TTCTCCACGCTCAACTACATCTC-3' and 5'-CAGCATCCGCGCCAGCACTGAGT-3'. PCR product was cloned into 5-alpha competent bacteria (New England Biolabs, cat. no. C2987) using a TOPO TA cloning kit (Thermo Fisher Scientific, cat. no. 450641) according to the manufacturer's instructions. After blue/white screening, a minimum of ten colonies were sequenced per THP-1 clone, and sequences were analysed using SeqMan (Lasergene DNASTAR). Nine independent THP-1 clones with out-of-frame mutations at the *SLC19A1* gRNA target site were selected for further experiments. These clones were all significantly less sensitive to CDN stimulation when compared to seven control clones that received a non-targeting gRNA (Fig. 2e).

shRNA knockdown. For shRNA knockdown experiments, shRNA sequences were cloned into the pLKO.1 lentiviral expression vector. Cells were transduced with lentivirus and selected using 2 μ g ml⁻¹ puromycin for at least 5 days. As controls, shRNAs targeting GFP (shRNA1; TRCN0000231753) and luciferase (shRNA2 TRCN0000231737) were used. Mouse *SLC19A1* targeting shRNA sequences: GCAGGTGACTAACGAGATCAT (shRNA 4), and CCGTATCTACTTCATATACTT (shRNA 5); human *SLC19A1* targeting shRNA (shRNA 9): CGACGGTGTTTCAGAAATGTGAA. All shRNA knockdowns were confirmed by real-time qPCR. Depletion of *SLC19A1* function was confirmed by showing decreased uptake of [³H]-methotrexate (see below and Extended Data Figs. 6l, 7c, g).

RT-qPCR. Cells were collected and washed in ice-cold PBS. Cells were transferred to RNase-free microcentrifuge tubes and RNA was isolated using the RNeasy mini kit (Qiagen, cat. no. 74104) including a DNase I step (Qiagen, cat. no. 79254). RNA concentration was measured by NanoDrop (Thermo Fisher), and 1 μ g of RNA was used as input for cDNA synthesis using the iScript cDNA synthesis kit (Bio-rad, cat. no. 1708890). cDNA was diluted to 20 ng μ l⁻¹ and 2.5 μ l per reaction was used as input for the qPCR reaction. qPCR reactions were set up using SSOFast EvaGreen Supermix (Bio-Rad, cat. no. 1725200) according to the manufacturer's recommendations, using 500 nM of each primer and following cycling conditions on a Bio-Rad C1000 Thermal Cycler: 2 min at 98 °C, 40 repeats of 2 s at 98 °C and 5 s at 55 °C. Primers used to amplify the *HPRT1*, *YWHAZ*, *CCL5*, *CXCL10*, *STING*, *IRF3*, *SLC19A1*, *SLC46A1* and *SLC46A3*-specific PCR products are listed in Supplementary Table 4. The housekeeping genes *HPRT1* and *YWHAZ* served as endogenous controls for human cDNA samples and *Gapdh* and *Ubc* served as endogenous control for mouse cDNA samples.

For quantification of human *IFNB1*, *OASL*, or *ISG15* mRNA, RNA was extracted with the Nucleospin RNA Isolation Kit (Machery-Nagel) and reverse-transcribed

with the iScript cDNA synthesis kit (Bio-Rad). TaqMan real-time qPCR assays were used for quantification of human *IFNB1* (Hs01077958_s1), human *OASL* (Hs00984387_m1), and human *ISG15* (Hs01921425_s1). *Actb* (Hs01060665_g1) served as an endogenous control.

Synthesis of [³²P]2'3'-cGAMP and [³²P]3'3'-CDA. Radiolabelled 2'3'-cGAMP was enzymatically synthesized by incubating 0.33 μ M α -[³²P]ATP (Perkin-Elmer) with 250 μ M unlabelled GTP, 1 μ g of interferon stimulatory DNA 10mer (provided by D. Stetson) and 1 μ M of recombinant His-tagged 2'3'-cGAMP synthase (cGAS) in binding buffer (40 mM Tris pH 7.5, 100 mM NaCl and 20 mM MgCl₂) at 37 °C overnight. The reaction was confirmed to have gone to completion by thin layer chromatography (TLC) analysis (Extended Data Fig. 6a, b). In brief, the 2'3'-cGAMP synthesis reaction was separated on Polygram CEL300 PEI TLC plates (Machery-Nagel) in buffer containing 1:1.5 (v/v) saturated (NH₄)₂SO₄ and 1.5 M NaH₂PO₄ pH 3.6. The TLC plates were then air-dried and exposed to a PhosphorImager screen for visualization using a Typhoon scanner (GE Healthcare Life Sciences). Next, the sample was incubated with HisPur Ni-NTA resin (Thermo Scientific) for 30 min to remove recombinant cGAS. The resultant slurry was transferred to a minispin column (Thermo Scientific) to elute crude [³²P]2'3'-cGAMP. Recombinant mSTING-CTD protein was used for further purification of synthesized [³²P]2'3'-cGAMP. mSTING-CTD (100 μ M) was bound to HisPur Ni-NTA resin and incubated with the remaining crude 2'3'-cGAMP synthesis reaction mixture for 30 min on ice. Following removal of the supernatant, the Ni-NTA resin was washed three times with cold binding buffer. The resin was then incubated with 100 μ l of binding buffer for 10 min at 95 °C, and transferred to a minispin column to elute [³²P]2'3'-cGAMP. The resulting STING-purified [³²P]2'3'-cGAMP was evaluated by TLC analysis and determined to be about 99% pure (Extended Data Fig. 6c).

Radiolabelled 3'3'-CDA was synthesized as previously described⁴³. In brief, 1 μ M α -[³²P]ATP (Perkin-Elmer) was incubated with 1 μ M of recombinant DisA in binding buffer at 37 °C overnight. The reaction mixture was boiled for 5 min at 95 °C and DisA was removed by centrifugation. Recombinant His-tagged RECON was then used to further purify the 3'3'-CDA reaction mixture. One-hundred micromolar His-tagged RECON was bound to HisPur Ni-NTA resin for 30 min on ice. The resin was washed three times with cold binding buffer and then incubated with 100 μ l of binding buffer for 5 min at 95 °C. The slurry was then transferred to a minispin column to elute [³²P]c-di-AMP. The purity of the radiolabelled 3'3'-CDA was assessed by TLC and determined to be about 98%.

Nucleotide-binding assays. The ability of radiolabelled 2'3'-cGAMP and 3'3'-CDA to bind recombinant STING was evaluated by differential radial capillary action of ligand assay (DRaCALA) analysis, as previously described⁴⁴ (Extended Data Fig. 6d). In brief, varying concentrations of recombinant STING were incubated with about 1 nM of radiolabelled CDN in binding buffer for 10 min at room temperature. The reaction mixtures were blotted on nitrocellulose membranes and air-dried for 15 min. The membranes were then exposed to a PhosphorImager screen and visualized using a Typhoon scanner.

NHS-methotrexate synthesis and affinity labelling. NHS-methotrexate was prepared as previously described⁴⁵. In brief, methotrexate (2.2 mg) was acidified by the addition of HCl and dried under vacuum. Next, acidified methotrexate, 1-ethyl-3-(3-dimethylaminopropyl) carbodiimide (EDC) (7.8 mg), and NHS (5.8 mg) were dissolved in 1 ml of anhydrous, tissue-culture grade dimethylsulfoxide and incubated for 2 h at 23 °C. The activated reagent was used immediately by incubating cells with 5 μ M NHS-methotrexate in RPMI 1640 medium (GIBCO) supplemented with 10 mM HEPES, 1 mM sodium pyruvate and 2 mM L-glutamine (Thermo Fisher) for 30 min at 37 °C. The cells were then recovered by centrifugation, washed twice in treatment medium and re-suspended in pre-warmed RPMI 1640 medium (GIBCO) containing 10% (v/v) heat-inactivated FBS (HyClone) and supplemented with 10 mM HEPES, 1 mM sodium pyruvate and 2 mM L-glutamine (Thermo Fisher) to a final cell density of 1×10^6 to 1×10^7 cells per ml.

Nucleotide-uptake assays. For transport assays, cells were collected by centrifugation and washed in Dulbecco's phosphate-buffered saline (DPBS) (Life Technologies). The cell pellets were re-suspended in pre-warmed RPMI 1640 medium (GIBCO) containing 10% heat-inactivated FBS (HyClone) and supplemented with 10 mM HEPES, 1 mM sodium pyruvate and 2 mM L-glutamine (Thermo Fisher) to a final cell density of 1×10^7 cells per ml. Uptake of 1 nM [³²P]2'3'-cGAMP and 3'3'-CDA was assayed in cell suspensions at 37 °C over the indicated time points. At the end of each time point, transport was quenched by the addition of cold DPBS. Cells were washed three times with cold DPBS, followed by lysis in 50 μ l of cold deionized water. The cell lysates were then transferred to 5 ml of liquid scintillation cocktail (National Diagnostics) and the associated radioactivity was measured by liquid scintillation counting using a LS6500 Liquid Scintillation Counter (Beckman Coulter). For each sample, [³²P]2'3'-cGAMP (counts per minute) was normalized to cell count (10^6 cells per sample). For competition experiments, cells were pre-incubated with indicated concentrations of 'cold' unlabelled ligand or inhibitor for 15 min before the addition of 1 nM 'hot'

[³²P]2′3′-cGAMP. Cells were then collected at the indicated time points and processed as described above.

2′3′-cGAMP was incorporated into THP-1 cells at a linear rate over at least three hours of incubation (Extended Data Fig. 6e), during which time the [³²P]2′3′-cGAMP was not hydrolyzed or modified (Extended Data Fig. 6f). 2′3′-cGAMP uptake was most efficient at a pH range of 7.5 to 8.0 in both THP-1 and U937 cells (Extended Data Fig. 6g, h), consistent with a neutral pH optimum for SLC19A1¹⁵.

[³H]-methotrexate uptake assays. Tritium-labelled methotrexate (Vitracat. no. VT 145) had a specific activity of 40.6 Ci/mmol. Uptake of [³H]-methotrexate in SLC19A1-knockdown and SLC19A1-overexpressing cells was performed in RPMI complete medium. [³H]-methotrexate competition assays were performed in MHS buffer (20 mM HEPES, 235 mM sucrose adjusted to pH 7.4 using MgO). Cells were washed and resuspended in the appropriate buffer to 4 × 10⁶ cells per ml. Cells (10⁶ per condition) were exposed to 12.3 nM [³H]-methotrexate (1.25 μCi) at 37°C and 5% CO₂ for the duration indicated in the figure legends. Cells were subsequently washed four times in ice cold PBS to stop uptake and remove extracellular [³H]-methotrexate. Cells were lysed in 250 μl ice cold water and 200 μl was mixed with 4 ml scintillation liquid. Fifty microlitres was used for protein quantification using the bicinchoninic acid (BCA) assay (Thermo Scientific cat. no. 23235). Radioactivity (counts per minute) was measured for 3 min per sample using liquid scintillation counting using a LS6500 Liquid Scintillation Counter (Beckman Coulter). Counts per minute were normalized to total protein. For competition assays, cells were incubated for 15 min at 37°C and 5% CO₂ with the indicated ligand in MHS buffer before addition of [³H]-methotrexate.

Enzyme-linked immunosorbent assay. Cells were stimulated with 2′3′-RR CDA (2 μg ml⁻¹) for 20 h. Supernatant was collected and centrifuged to remove cells. CXCL10 was quantified in the supernatant using the CXCL10 ELISA kit (BioLegend cat. no. 439904) according to the manufacturer's recommendations.

Digitonin permeabilization. Cells were counted, washed and resuspended to 2 × 10⁶ cells per ml. Cells (10⁶ per condition) were permeabilized using 5 μg ml⁻¹ digitonin (Sigma cat. no. D-141; stock dissolved in H₂O) and stimulated with 2′3′-RR CDA (10 μg ml⁻¹) and the indicated SLC19A1 (competitive) inhibitor for 2 h at 37°C and 5% CO₂. Cells were subsequently washed in ice cold PBS, lysed in RIPA buffer and used for western blot protein analysis.

Protein expression and purification. Full-length human SLC19A1 cDNA with a C-terminal 8 × His-tag was subcloned into a dual promoter lentiviral vector (see above). Recombinant His-tagged SLC19A1 was expressed using a FreeStyle 293 Expression System. In brief, 293F cells (1 × 10⁶ cells per ml) grown in FreeStyle 293 medium supplemented with GlutaMax (GIBCO) were transfected with the SLC19A1 expression construct (1 μg plasmid DNA per ml of cells) using PEI transfection reagent. Transfected cells were grown for 72 h in a shaking incubator at 37°C in 5% CO₂. Three days after transfection, the cells were collected by centrifugation and washed in DBPS. Cell pellets were then re-suspended in lysis buffer (25 mM Tris pH 8.0, 150 mM NaCl, 1 mM phenylmethylsulfonyl fluoride) supplemented with HALT Protease and Phosphatase Inhibitor Cocktail (Thermo Scientific) and lysed by sonication. The cell lysate was supplemented with 2% (w/v) *n*-dodecyl-β-D-maltoside (DDM) and rotated for 2 h at 4°C. The cell lysates were centrifuged at 15,000 r.p.m. for 1 h at 4°C to remove cell debris, and the detergent-soluble fraction was incubated with HisPur Ni-NTA resin for 1 h at 4°C. The resin was washed with 100 column volumes of wash buffer (25 mM Tris pH 6.0, 150 mM NaCl, 30 mM imidazole, 5% glycerol (v/v) and 0.05% DDM (w/v)), and bound proteins were eluted in elution buffer (25 mM Tris pH 6.0, 150 mM NaCl, 300 mM imidazole, 5% glycerol (v/v) and 0.05% DDM (w/v)). The resulting proteins were analysed by SDS-PAGE followed by Coomassie staining and immunoblotting to confirm expression and purification of His-tagged SLC19A1.

Recombinant cGAS, DisA, mSTING-CTD, and mRECON were expressed and purified as previously described^{43,44,46}. In brief, plasmids for cGAS, DisA, mSTING-CTD, and mRECON expression were transformed into Rosetta (DE3) pLys chemically competent cells. Overnight cultures of the resulting transformed bacteria were inoculated into 1.5 l of LB broth at a 1:100 dilution. Bacterial cultures were grown at 37°C to OD₆₀₀ 0.5 followed by overnight induction at 18°C with 0.5 mM isopropyl β-D-1-thiogalactopyranoside. Cells were collected and lysed in PBS supplemented with 1 mM PMSF and soluble protein was purified using nickel-affinity chromatography followed by gel-filtration chromatography (S-300, GE Healthcare). After SDS-PAGE analysis, the purified proteins were concentrated in storage buffer (40 mM Tris pH 7.5, 100 mM NaCl, 20 mM MgCl₂ and 25% glycerol (v/v)) and stored at -80°C.

Synthesis of 2′3′-cGAMP Sepharose. 2′3′-cGAMP was enzymatically synthesized using recombinant cGAS as previously described^{47,44}. Approximately, 100 mg of purified 2′3′-cGAMP was dissolved in PBS to 200 μM. The pH of the solution was adjusted to 7.5 with NaOH, and the resulting solution was added directly to washed epoxy-activated Sepharose and incubated at 56°C for 2 days. The Sepharose was washed and the absorbance spectrum of 50% slurry was measured to ensure nucleotide coupling. HPLC analysis of the remaining uncoupled nucleotide ensured no

degradation of 2′3′-cGAMP occurred during the two-day incubation. The remaining epoxy groups were blocked with ethanolamine following the instructions provided by GE. In parallel with this blocking step, fresh epoxy-activated Sepharose was also treated with ethanolamine to generate control resin.

2′3′-cGAMP pulldowns. Following nickel affinity purification, recombinant His-tagged SLC19A1 was incubated with 100 μl of ethanolamine- or 2′3′-cGAMP-conjugated Sepharose beads for 4 h at 4°C with rotation, as previously described^{44,46}. Beads were washed three times with wash buffer (25 mM Tris pH 6.0, 150 mM NaCl, 5% glycerol (v/v) and 0.05% DDM (w/v)), and bound proteins were eluted by boiling in SDS-PAGE sample loading buffer for 5 min at 95°C. The soluble fraction was then removed and analysed by SDS-PAGE followed by Coomassie blue staining and immunoblotting. As a positive control, recombinant His-tagged mSTING-CTD was incubated with ethanolamine- or 2′3′-cGAMP-conjugated Sepharose beads, as described above (Fig. 4g, Extended Data Fig. 8d). Beads were washed three times with binding buffer, and then boiled in SDS-PAGE sample loading buffer for 5 min at 95°C. The soluble fraction was then analysed by SDS-PAGE followed by Coomassie blue staining.

Cell lysis and immunoblotting. For immunoblotting of SLC19A1, cells were lysed and proteins were separated by SDS-PAGE as described in '2′3′-cGAMP pulldowns'. Proteins separated by SDS-PAGE were transferred onto nitrocellulose membranes (Bio-Rad) at 30 V overnight at 4°C. Membranes were then air-dried for 1 h and blocked in 5% Blotto, non-fat milk (NFM, Santa Cruz Biotechnology) in 1 × TBS. Membranes were probed in 5% bovine serum albumin (Fisher) in 1 × TBS-T with SLC19A1 Picoband antibody (Boster Bio).

For protein detection using all other antibodies, cells were counted, washed with PBS and lysed in RIPA buffer (25 mM Tris-HCl pH 7.5, 150 mM NaCl, 1 mM EDTA, 1% NP-40 and 0.1% SDS) including cOmplete ULTRA protease inhibitors (Sigma-Aldrich cat. no. 05892791001), phosphatase inhibitors (Biomake, cat. no. B15001) and 50 mM DTT. Cell lysates were mixed with 4 × NuPage LDS sample buffer (Invitrogen cat. no. NP0007), pulse sonicated and incubated at 75°C for 5 min. Lysates were loaded onto Bolt 4–12% Bis-Tris Plus SDS-PAGE gels (Invitrogen cat. no. NW04125BOX). Proteins separated by SDS-PAGE were transferred onto Immobilon-FL PVDF membranes (EMD Millipore) at 100 V for 1 h at 4°C. Membranes were blocked in 4% NFM, and probed in 1% NFM overnight at 4°C with primary antibody. Membranes were subsequently washed three times in 1 × TBS-T and probed with secondary antibody for 1 h at room temperature while protected from light. Membranes were washed two times in TBS-T, once in TBS and blots were imaged using an Odyssey CLx System (LI-COR).

Mice. Male and female C57BL/6J mice (4–20 weeks old) were obtained from The Jackson Laboratory. All of the mice were maintained in specific-pathogen-free conditions by the Department of Comparative Medicine at the University of Washington School of Medicine or at the University of California, Berkeley. All experimental procedures using mice complied with all relevant ethical regulations and were approved by the Institutional Animal Care and Use Committee of the University of Washington or the University of California, Berkeley, and were conducted in accordance with institutionally approved protocols and guidelines for animal care and use.

Isolation of mouse splenocytes and bone-marrow-derived dendritic cells and macrophages. For isolation of mouse splenocytes, spleens were removed from mice, strained through a 70-μm cell strainer, and homogenized into a single-cell suspension using ice-cold PBS supplemented with 3% FCS. Red blood cells were lysed by resuspending spleen cells in Red Blood Cell Lysing Buffer (Sigma) and incubating on ice for 10 min. Splenocytes were washed, resuspended in RPMI 1640 medium (GIBCO) supplemented with 10% (v/v) heat-inactivated FBS (HyClone), 10 mM HEPES, 1 mM sodium pyruvate, 2 mM L-glutamine (Thermo Fisher), 100 U ml⁻¹ penicillin and 100 μg ml⁻¹ streptomycin, and used immediately for [³²P]2′3′-cGAMP uptake assays.

For generation of bone-marrow-derived macrophages (BMDs) and dendritic cells (BMDCs), bones from the hind legs were removed and crushed to release the bone marrow. Bone marrow was washed in complete RPMI medium and filtered using a 70-μm cell strainer. Cells were incubated in ammonium-chloride-potassium buffer for 2 min to remove red blood cells. Cells were subsequently resuspended in RPMI 1640 supplemented with 10% (v/v) heat-inactivated FBS (HyClone), 10 mM HEPES, 1 mM sodium pyruvate, 2 mM L-glutamine (Thermo Fisher), 100 U ml⁻¹ penicillin, 100 μg ml⁻¹ streptomycin, and 5 ng ml⁻¹ GM-CSF (Preprotech, cat. no. 315-03) to generate BMDCs or M-CSF conditioned medium to generate macrophages. Cells were transduced with shRNA-encoding lentiviruses on day 2 and 3 after bone-marrow isolation, and selected using 7 μg ml⁻¹ puromycin for 3 days starting at day 5 after bone marrow isolation. Medium was refreshed every other day. Nine days after bone marrow isolation, non-adherent BMDCs or adherent BMD cells were collected. Cells were stimulated with 5 μg ml⁻¹ 2′3′-RR CDA for 5 h before RNA extraction.

Isolation of human peripheral blood mononuclear cells. Whole blood from healthy, human donors was collected in 10-ml EDTA blood tubes (Beckton

Dickinson) from healthy adults with written informed consent. Bulk PBMCs were isolated using SepMate tubes (STEMCELL Technologies) according to the manufacturer's instructions. The remaining cells were washed in PBS, resuspended in RPMI 1640 medium (GIBCO) supplemented with 10% (v/v) heat-inactivated FBS (HyClone), 10 mM HEPES, 1 mM sodium pyruvate, 2 mM L-glutamine (Thermo Fisher), 100 U ml⁻¹ penicillin, 100 µg ml⁻¹ streptomycin, and used immediately for [³²P]2'3'-cGAMP uptake assays. The isolation of primary human cells complied with all relevant ethical regulations and was conducted under a protocol from K. B. Elkon which was approved by the University of Washington Institutional Review Board.

Reporting summary. Further information on research design is available in the Nature Research Reporting Summary linked to this paper.

Code availability

The CRISPRi screen sequences were analysed using the Python-based ScreenProcessing pipeline. This custom code is available at <https://github.com/mhorlbeck/ScreenProcessing>.

Data availability

Raw sequencing data from the CRISPRi screens are available at NCBI Gene Expression Omnibus under accession number GSE134371.

31. van de Weijer, M. L. et al. A high-coverage shRNA screen identifies TMEM129 as an E3 ligase involved in ER-associated protein degradation. *Nat. Commun.* **5**, 3832 (2014).
32. Zhao, R. et al. Impact of the reduced folate carrier on the accumulation of active thiamin metabolites in murine leukemia cells. *J. Biol. Chem.* **276**, 1114–1118 (2001).
33. Zhao, R., Gao, F. & Goldman, I. D. Reduced folate carrier transports thiamine monophosphate: an alternative route for thiamine delivery into mammalian cells. *Am. J. Physiol. Cell Physiol.* **282**, C1512–C1517 (2002).
34. Visentin, M., Zhao, R. & Goldman, I. D. Augmentation of reduced folate carrier-mediated folate/antifolate transport through an antiport mechanism with 5-aminoimidazole-4-carboxamide riboside monophosphate. *Mol. Pharmacol.* **82**, 209–216 (2012).
35. Henderson, G. B. & Zevely, E. M. Anion exchange mechanism for transport of methotrexate in L1210 cells. *Biochem. Biophys. Res. Commun.* **99**, 163–169 (1981).
36. Hamblett, K. J. et al. SLC46A3 is required to transport catabolites of noncleavable antibody maytansine conjugates from the lysosome to the cytoplasm. *Cancer Res.* **75**, 5329–5340 (2015).
37. van Diemen, F. R. et al. CRISPR/Cas9-mediated genome editing of herpesviruses limits productive and latent infections. *PLoS Pathog.* **12**, e1005701 (2016).
38. Horlbeck, M. A. et al. Compact and highly active next-generation libraries for CRISPR-mediated gene repression and activation. *eLife* **5**, 1–20 (2016).
39. Kampmann, M., Bassik, M. C. & Weissman, J. S. Functional genomics platform for pooled screening and generation of mammalian genetic interaction maps. *Nat. Protoc.* **9**, 1825–1847 (2014).
40. Gilbert, L. A. et al. Genome-scale CRISPR-mediated control of gene repression and activation. *Cell* **159**, 647–661 (2014).
41. Kampmann, M., Bassik, M. C. & Weissman, J. S. Integrated platform for genome-wide screening and construction of high-density genetic interaction maps in mammalian cells. *Proc. Natl Acad. Sci. USA* **110**, E2317–E2326 (2013).
42. Sadlish, H., Williams, F. M. R. & Flintoff, W. F. Functional role of arginine 373 in substrate translocation by the reduced folate carrier. *J. Biol. Chem.* **277**, 42105–42112 (2002).
43. Huynh, T. N. et al. An HD-domain phosphodiesterase mediates cooperative hydrolysis of c-di-AMP to affect bacterial growth and virulence. *Proc. Natl Acad. Sci. USA* **112**, E747–E756 (2015).
44. Sureka, K. et al. The cyclic dinucleotide c-di-AMP is an allosteric regulator of metabolic enzyme function. *Cell* **158**, 1389–1401 (2014).
45. Henderson, G. B. & Zevely, E. M. Affinity labeling of the 5-methyltetrahydrofolate/methotrexate transport protein of L1210 cells by treatment with an N-hydroxysuccinimide ester of [3H]methotrexate. *J. Biol. Chem.* **259**, 4558–4562 (1984).
46. McFarland, A. P. et al. Sensing of bacterial cyclic dinucleotides by the oxidoreductase RECON promotes NF-κB activation and shapes a proinflammatory antibacterial state. *Immunity* **46**, 433–445 (2017).

Acknowledgements We thank L. Zhang and E. Seidel for laboratory and technical assistance, H. Nolla and A. Valeros for assistance with cell sorting, the UC Berkeley High Throughput Screening Facility for preparation of gRNA lentivirus, A. P. McFarland for assistance in the isolation of primary cells from mice, S. L. McDevitt for assistance with deep sequencing, J. An and K. Elkon for assistance in the collection and isolation of primary peripheral blood leukocytes from healthy, human volunteers, and Raulet laboratory members, R. Vance, M. DuPage, M. van Gent, J. Thorner and A. van Elsas for helpful discussions. R.D.L. is a Cancer Research Institute Irvington Fellow supported by the Cancer Research Institute. D.H.R. is supported by NIH grants R01-AI113041 and R01-CA093678. B.G.G. is supported by the IGI-AstraZeneca Postdoctoral Fellowship. J.J.W. is supported by the Pew Scholars Program in the Biomedical Sciences, the Lupus Research Alliance and NIH grant 1R21AI137758-01. S.A.Z. is supported by grants from the University of Washington/Fred Hutchinson Cancer Research Center Viral Pathogenesis Training Program (AI083203), the University of Washington Medical Scientist Training Program (GM007266) and the Seattle ARCS foundation. J.E.C. is supported by the National Institute of Health New Innovator Awards (DP2 HL141006), the Li Ka Shing Foundation and the Heritage Medical Research Institute. This work employed the Vincent J. Coates Genomics Sequencing Laboratory at UC Berkeley, supported by NIH S10 Instrumentation Grants S10 OD018174, S10RR029668 and S10RR027303.

Author contributions R.D.L., S.A.Z. and N.E.G. performed and analysed the experiments; L.O., S.M.M. and G.E.K. assisted with the experiments; S.K.W. and B.G.G. analysed the deep-sequencing data and advised on the screen design; R.D.L., S.A.Z., B.G.G., J.E.C., J.J.W. and D.H.R. designed the experiments and R.D.L., S.A.Z., J.J.W. and D.H.R. prepared the manuscript. All authors critically read the manuscript.

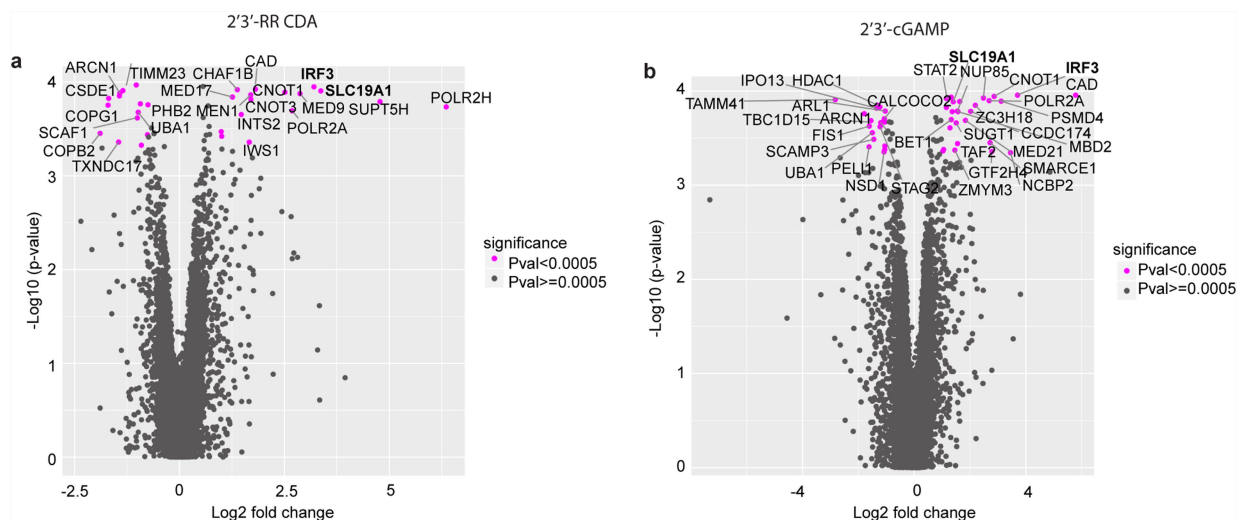
Competing interests D.H.R. is a co-founder of Dragonfly Therapeutics and served or serves on the scientific advisory boards of Dragonfly, Aduro Biotech, and Ignite Immunotherapy; he has a financial interest in all four companies and could benefit from commercialization of the results of this research. S.M.M. is, and G.E.K. was, an employee of Aduro Biotech.

Additional information

Supplementary information is available for this paper at <https://doi.org/10.1038/s41586-019-1553-0>.

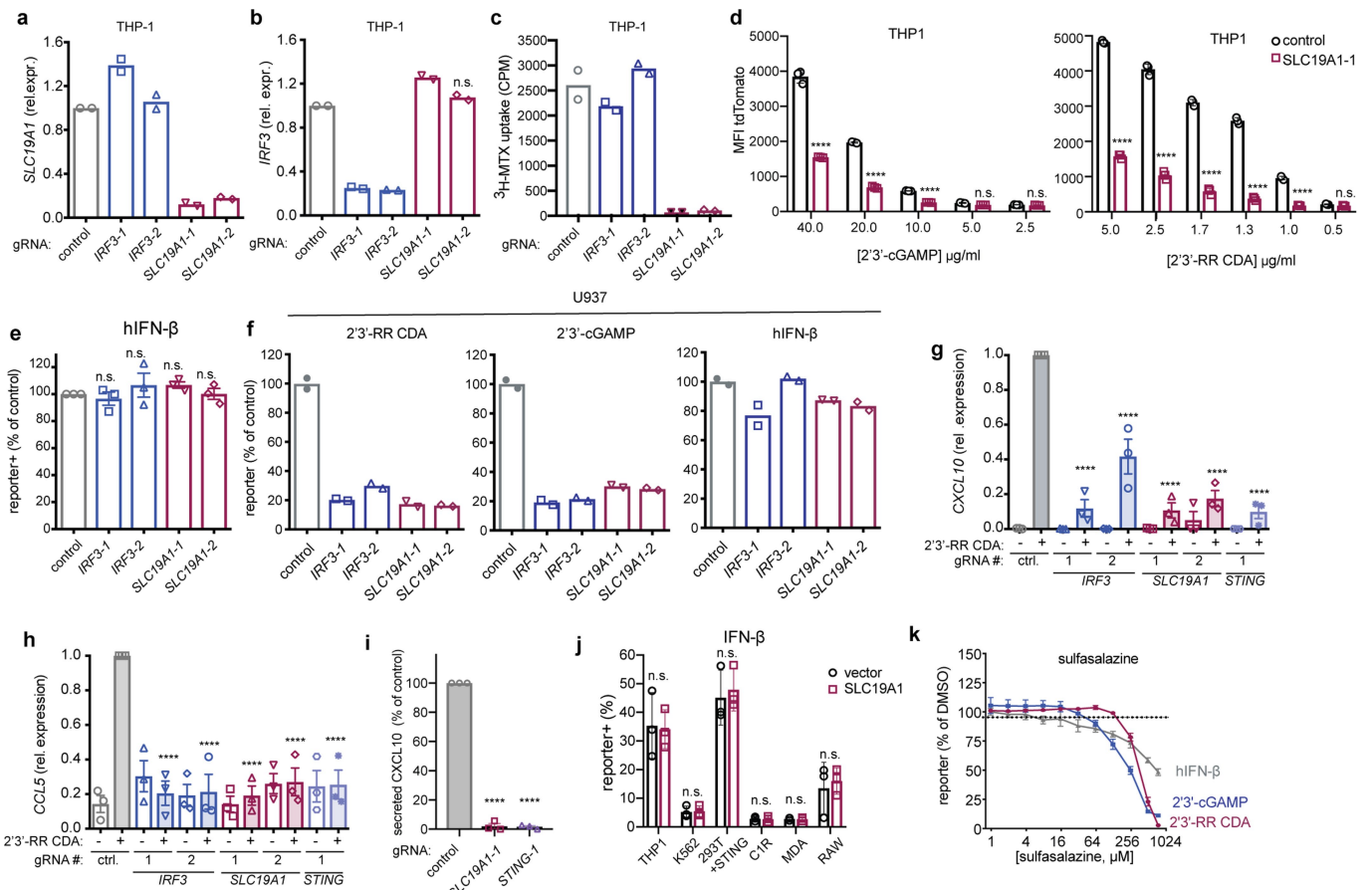
Correspondence and requests for materials should be addressed to D.H.R.

Reprints and permissions information is available at <http://www.nature.com/reprints>.



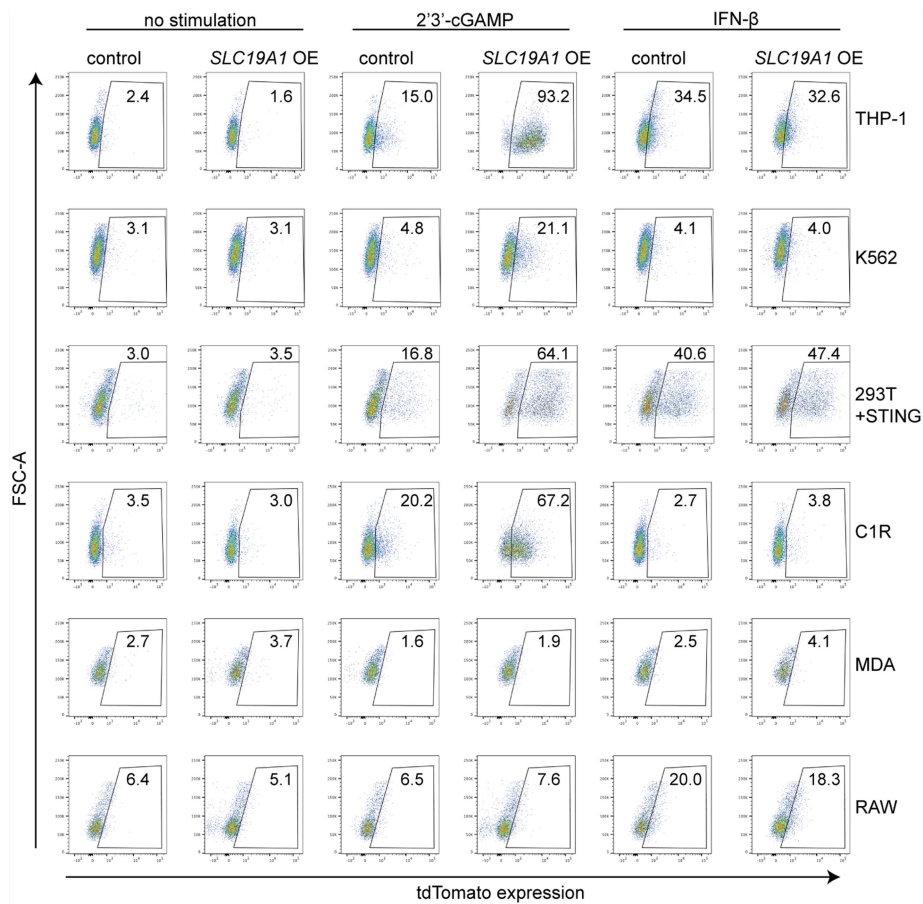
Extended Data Fig. 2 | Results of genome-wide CRISPRi screens for host factors crucial for CDN stimulation. a, b. Volcano plots of the gRNA-targeted genes enriched or depleted in the tdTomato reporter-low versus reporter-high groups after stimulation with 2'3'-RR CDA (a),

or 2'3'-cGAMP (b). Each panel represents the combined results of two independent screens. Calculations of phenotypes and Mann-Whitney *P* values were performed as described in Methods.



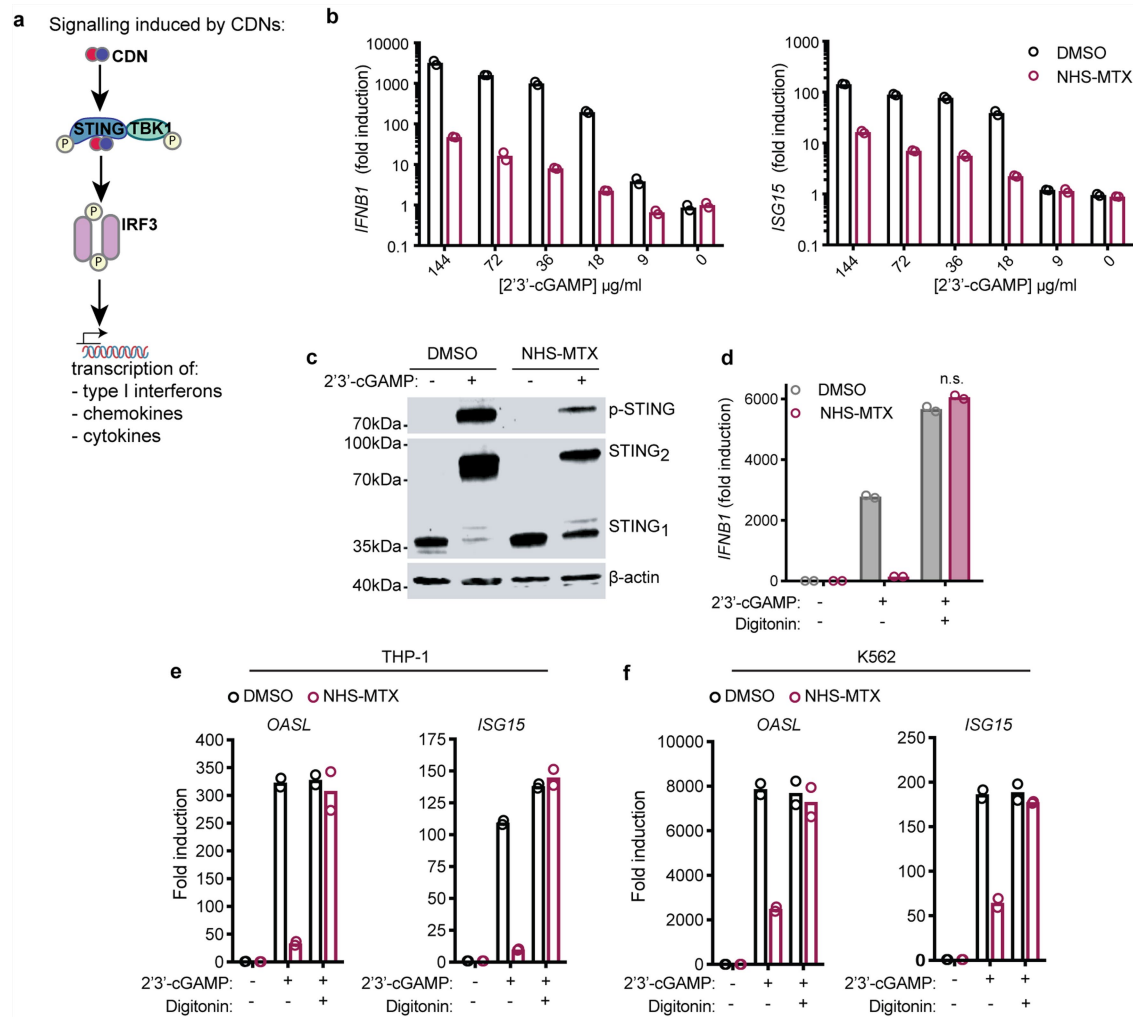
Extended Data Fig. 3 | SLC19A1 is critical for CDN-induced gene expression. **a**, **b**, mRNA expression levels of *SLC19A1* (**a**) or *IRF3* (**b**) in THP-1 cells expressing a CRISPRi vector and a control non-targeting gRNA or gRNAs targeting *IRF3* or *SLC19A1* (two gRNAs each). **c**, THP-1 cells described in **a** and **b** were exposed to [³H]-methotrexate. After 1 h, radioactivity (in counts per minute, cpm) in lysates of cell pellets was measured. Counts were normalized to protein concentrations in the lysate. **d**, THP-1 cells expressing a control gRNA or *SLC19A1*-targeting gRNA were exposed to indicated concentrations of 2'3'-RR CDA or 2'3'-cGAMP. After 20 h, the mean fluorescence intensity (MFI) of tdTomato was quantified by flow cytometry. **e**, THP-1 cells expressing the indicated CRISPRi gRNAs or non-targeting gRNA (control), were stimulated with IFN- β (100 ng ml⁻¹). After 18–22 h, tdTomato expression was quantified as in Fig. 2a. **f**, U937 cells expressing the indicated CRISPRi gRNAs or non-targeting gRNA (control), were stimulated with 2'3'-RR CDA (1.67 μ g ml⁻¹), 2'3'-cGAMP (15 μ g ml⁻¹) or IFN- β (100 ng ml⁻¹). After 18–22h, tdTomato expression was quantified as in Fig. 2a. **g**, **h**, Induction of *CXCL10* mRNA (**g**) or *CCL5* mRNA (**h**) in control (non-targeting

gRNA) THP-1 cells or THP-1 cells expressing the indicated CRISPRi gRNAs after 5 h stimulation with 5 μ g ml⁻¹ 2'3'-RR CDA. **i**, *CXCL10* protein expression in the supernatant of indicated gRNA-expressing THP-1 cells after exposure to 2 μ g ml⁻¹ 2'3'-RR CDA for 20 h. **j**, Various cell lines expressing a control vector or an *SLC19A1* expression vector were stimulated with IFN- β (100 ng ml⁻¹). After 18–22 h, tdTomato expression was quantified as in Fig. 2a. **k**, THP-1 cells were incubated with increasing concentrations of the non-competitive inhibitor sulfasalazine or DMSO as vehicle control, before stimulation with 2'3'-RR CDA (1.25 μ g ml⁻¹), 2'3'-cGAMP (15 μ g ml⁻¹) or IFN- β (100 ng ml⁻¹). After 18–22 h, tdTomato expression was quantified as in Fig. 2a. The data were normalized to the DMSO controls. In **a**–**c** and **e**–**f**, mean of $n = 2$ biological replicates are shown. In **d**, **g**–**k**, mean \pm s.e.m. of $n = 3$ biological replicates are shown. Statistical analyses were performed to compare each cell line to the control using a one-way ANOVA followed by post hoc Dunnett's test (**d**, **g**–**i**) or two-way ANOVA followed by uncorrected Fisher's least significant difference tests (**j**). **** $P \leq 0.0001$; n.s., not significant.



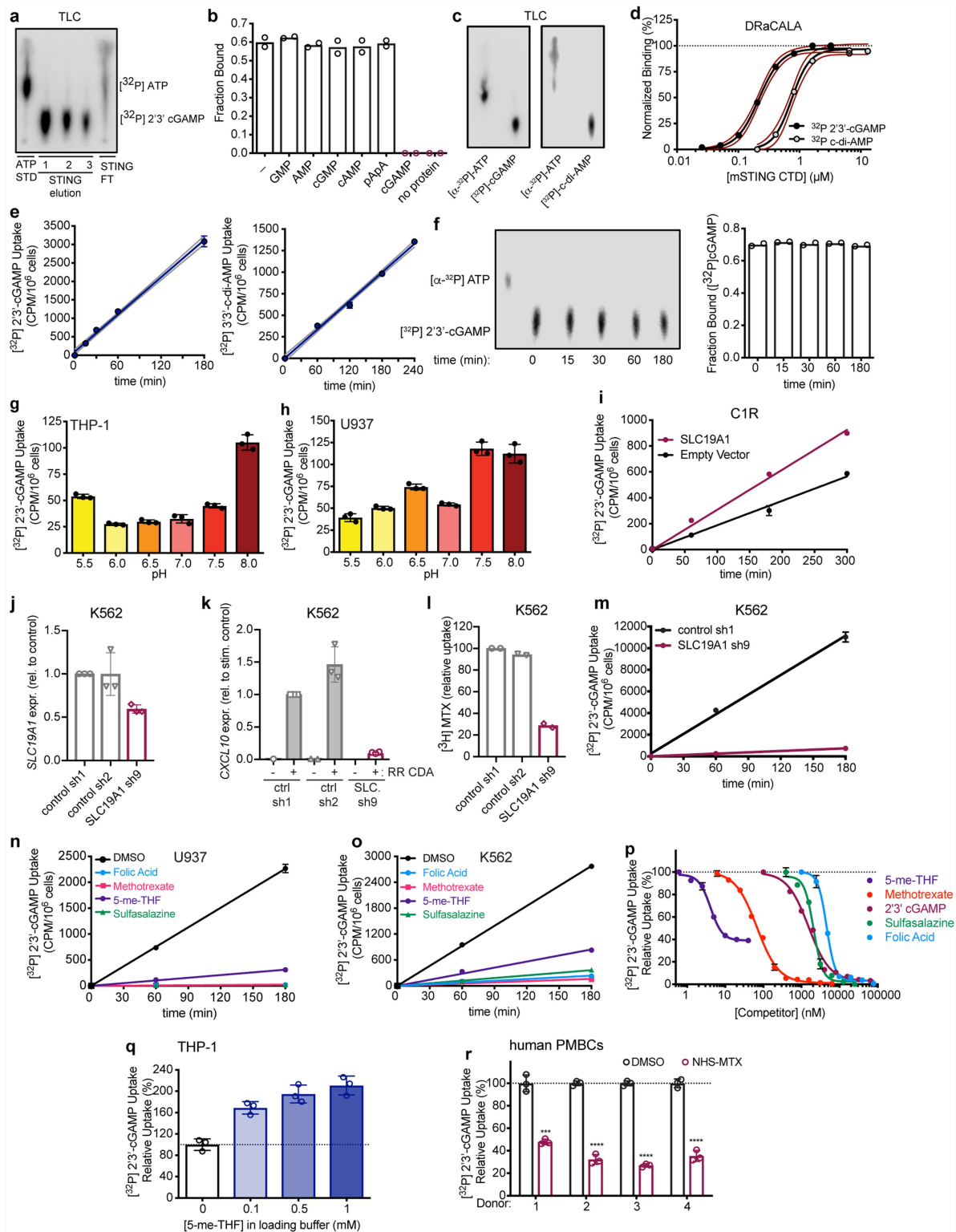
Extended Data Fig. 4 | *SLC19A1* overexpression increases the response to CDNs in various cell lines. Various cell lines expressing a control vector or an *SLC19A1* expression vector (*SLC19A1* OE) stimulated with 2'3'-cGAMP ($10 \mu\text{g ml}^{-1}$) (e) or IFN- β (100 ng ml^{-1}) (or 100 ng ml^{-1})

mouse IFN- β in the case of RAW cells). After 20 h, reporter expression was quantified by flow cytometry. Representative flow plots of $n = 3$ biological replicates shown in Fig. 2f and Extended Data Fig. 3j.



Extended Data Fig. 5 | Covalent inhibition of SLC19A1 by NHS-methotrexate blocks STING activation. **a**, Schematic overview of CDN-induced phosphorylation (P) of STING and downstream effectors TBK1 and IRF3. **b**, THP-1 monocytes pre-treated with DMSO or NHS-methotrexate (5 μ M) were treated with varying concentrations of 2'3'-cGAMP for 4 h, and the amounts of *IFNB1* or *ISG15* transcripts were measured by RT-qPCR. **c**, Semi-native PAGE and immunoblot analysis of STING dimerization and phosphorylation in DMSO and NHS-methotrexate (5 μ M) pre-treated THP-1 monocytes stimulated with 100 μ M 2'3'-cGAMP for 4 h. For gel source data, see Supplementary Fig. 1.

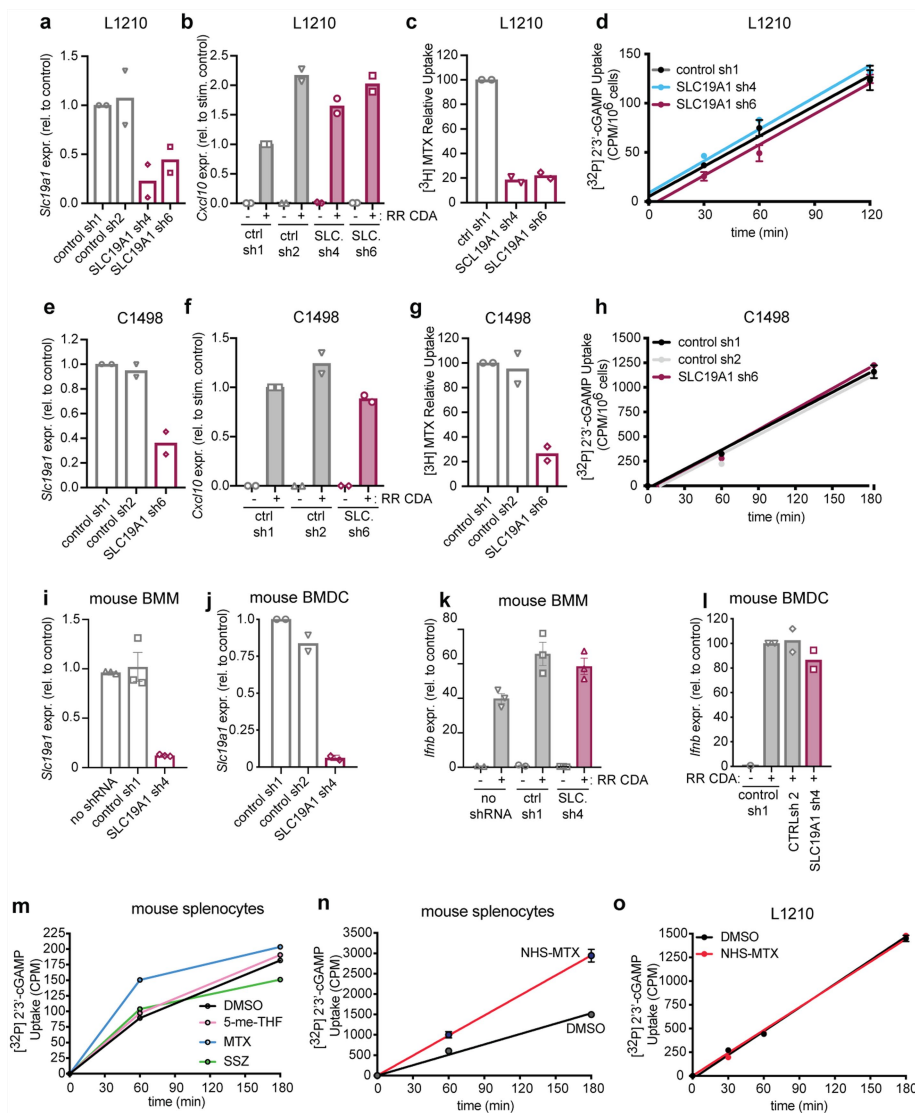
d, DMSO and NHS-methotrexate (5 μ M)-treated THP-1 monocytes were treated with 100 μ M 2'3'-cGAMP in the presence and absence of digitonin (5 μ g ml⁻¹) for 4 h and the induction of *IFNB1* mRNA was measured by RT-qPCR. **e**, **f**, DMSO and NHS-methotrexate (5 μ M) pre-treated THP-1 monocytes (**e**) or K562 cells (**f**) were stimulated for 4 h with 100 μ M 2'3'-cGAMP, or not, in the presence or absence of digitonin (5 μ g ml), and the induction of *OASL* and *ISG15* mRNA was measured by RT-qPCR. In **b**, **d-f**, data are mean of $n = 2$ technical replicates and are representative of 3 independent experiments with similar results. In **c**, data are representative of three independent experiments with similar results.



Extended Data Fig. 6 | See next page for caption.

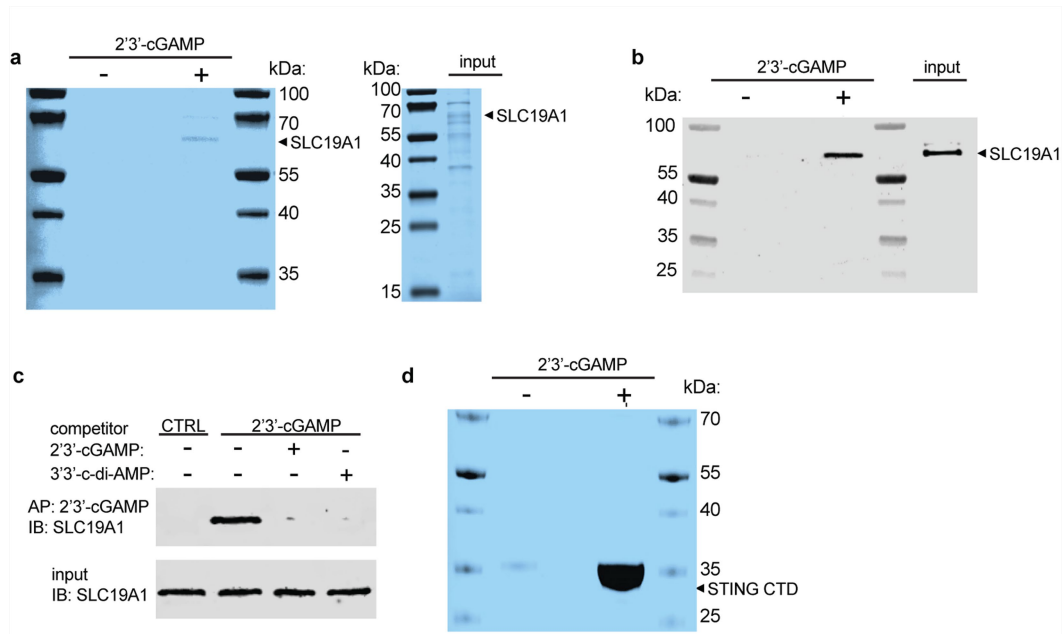
Extended Data Fig. 6 | SLC19A1 is critical for CDN uptake in human cell lines and primary cells. **a**, TLC analysis of [32 P]ATP standard (STD) and enzymatically synthesized [32 P]2′3′-cGAMP (2′3′-cGAMP was purified on STING resin). Unbound nucleotides flowed through the resin (STING FT). Following four washes, the bound [32 P]2′3′-cGAMP was eluted over three fractions. **b**, DRaCALA binding analysis of [32 P]2′3′-cGAMP to STING C-CTD in the presence of competing unlabelled nucleotides (200 μ M). **c**, TLC analysis of [32 P]ATP and enzymatically synthesized [32 P]2′3′-cGAMP and [32 P]-c-di-AMP. **d**, Binding titration of [32 P]2′3′-cGAMP or [32 P]-c-di-AMP to mSTING CTD, determined with DRaCALA assays. Red lines represent the 95% confidence interval for the nonlinear regression. **e**, Time course of [32 P]2′3′-cGAMP (left) or [32 P]3′3′-CDA (right) uptake in THP-1 monocytes. **f**, TLC analysis (left) and STING-binding (DRaCALA) (right) of [32 P]ATP standard, or [32 P]2′3′-cGAMP recovered from supernatants of THP-1 monocytes at the indicated time points. **g, h**, Effect of cell culture medium pH on [32 P]2′3′-cGAMP uptake in THP-1 monocytes (**g**) or U937 monocytes (**h**). **i**, Time course of [32 P]2′3′-cGAMP uptake by CIR cells transduced with empty vector or *SLC19A1* expression vector. **j**, mRNA expression levels of *SLC19A1* (SLC.) in K562 cells expressing control shRNAs (sh1 and sh2) or an *SLC19A1*-targeting shRNA (sh9). **k**, mRNA expression levels of *CXCL10* in K562 cells described in **j**, stimulated with 5 μ g ml $^{-1}$ 2′3′-RR CDA (RR CDA) for 5 h. **l**, [3 H]-methotrexate uptake in K562 cells described in **j**, 1 h after exposure to [3 H]-methotrexate. **m**, Time course

of [32 P]2′3′-cGAMP uptake in K562 cells described in **j**. **n**, Time course of [32 P]2′3′-cGAMP uptake in U937 monocytes in the presence or absence of 500 μ M competing, unlabelled (anti-)folates and sulfasalazine. **o**, Time course of [32 P]2′3′-cGAMP uptake in K562 cells in the presence or absence of 500 μ M competing, unlabelled (anti-)folates or sulfasalazine. **p**, Competition uptake assay of [32 P]2′3′-cGAMP uptake in THP-1 cells in the presence of varying concentrations of competing, unlabelled 5-me-THF ($IC_{50} = 4.10 \pm 0.16$ nM), methotrexate ($IC_{50} = 54.83 \pm 5.08$ nM), 2′3′-cGAMP ($IC_{50} = 1.89 \pm 0.11$ μ M), sulfasalazine ($IC_{50} = 2.06 \pm 0.17$ μ M), and folic acid ($IC_{50} = 4.79 \pm 0.08$ μ M). **q**, *Trans*-stimulation of [32 P]2′3′-cGAMP influx in THP-1 cells by 5-me-THF. Cells were preloaded with indicated concentrations of 5-me-THF for 30 min. Cells were washed and incubated with [32 P]2′3′-cGAMP for one hour. **r**, Normalized [32 P]2′3′-cGAMP uptake after 1 h in DMSO or NHS-methotrexate (5 μ M)-treated human PBMCs from four healthy donors. In **a, c**, data are representative of three independent experiments with similar results. In **b**, data are mean of $n = 2$ technical replicates and are representative of 3 independent experiments. In **d, f**, data are mean of $n = 2$ technical replicates and are representative of 2 independent experiments. In **e, m**, data are mean \pm s.d. of $n = 3$ technical replicates and are representative of 3 independent experiments. In **g–i** and **n–r**, data are means \pm s.d. of $n = 3$ technical replicates and are representative of 2 independent experiments. In **j, k**, data are mean \pm s.e.m. of $n = 3$ biologically independent experiments. In **l**, data are mean of $n = 2$ biologically independent experiments.



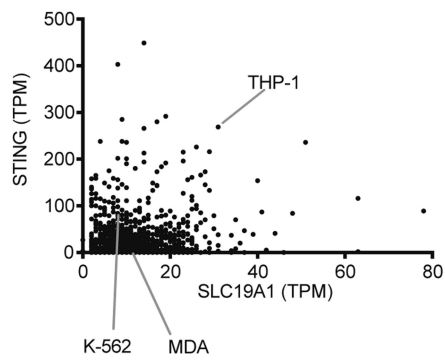
Extended Data Fig. 7 | SLC19A1 expression or inhibition has no effect on CDN uptake and signalling in mouse cells. **a**, mRNA expression levels of *Slc19a1* in mouse L1210 cells expressing control shRNAs (sh1 and sh2) or *Slc19a1*-targeting shRNA (sh4 and sh6). **b**, mRNA expression levels of *Cxcl10* in L1210 cells described in **a** stimulated with $5 \mu\text{g ml}^{-1}$ 2'3'-RR CDA (RR CDA) for 5 h. **c**, [³H]-methotrexate uptake in L1210 cells described in **a** 1 h after exposure to [³H]-methotrexate. **d**, Time course of [³²P]2'3'-cGAMP uptake in L1210 cells described in **a**. **e**, mRNA expression levels of *Slc19a1* in mouse C1498 cells expressing control shRNAs (sh1 and sh2) or *Slc19a1*-targeting shRNA (sh6). **f**, mRNA expression levels of *Cxcl10* in the C1498 cells described in **e**, stimulated with $5 \mu\text{g ml}^{-1}$ 2'3'-RR CDA (CDN) for 5 h. **g**, [³H]-methotrexate uptake in C1498 cells described in **e** 1 h after exposure to [³H]-methotrexate. **h**, Time course of [³²P]2'3'-cGAMP uptake in C1498 cells transduced with a non-targeting control shRNA or *Slc19a1* shRNA. **i**, **j**, mRNA expression levels of *Slc19a1* in mouse BMMs (**i**) or BMDCs (**j**) not

transduced or transduced with control shRNAs (sh1 and 2) or an shRNA targeting *Slc19a1*. **k**, **l**, mRNA expression of the *Cxcl10* in cells described in **i**, **j** stimulated with $5 \mu\text{g ml}^{-1}$ 2'3'-RR CDA (CDN) for 5 h. **m**, Time course of [³²P]2'3'-cGAMP uptake in primary mouse splenocytes in the presence and absence of 500 μM competing, unlabelled (anti-) folates and sulfasalazine. **n**, Time course of [³²P]2'3'-cGAMP uptake in primary mouse splenocytes pretreated or not with NHS-methotrexate (5 μM). **o**, Time course of [³²P]2'3'-cGAMP uptake in L1210 cells pretreated or not with NHS-methotrexate (5 μM). In **a**–**c**, **e**–**g**, **j**, **l**, data are mean of $n = 2$ biologically independent experiments. In **d**, **h**, **i**, **k**, **n**, **o**, data are mean \pm s.d. of $n = 3$ technical replicates and are representative of 2 independent experiments. In **m**, data are mean of $n = 2$ technical replicates and are representative of 2 independent experiments. In time-course experiments (**d**, **h**, **m**–**o**), data are presented as counts per minute normalized to cell count.

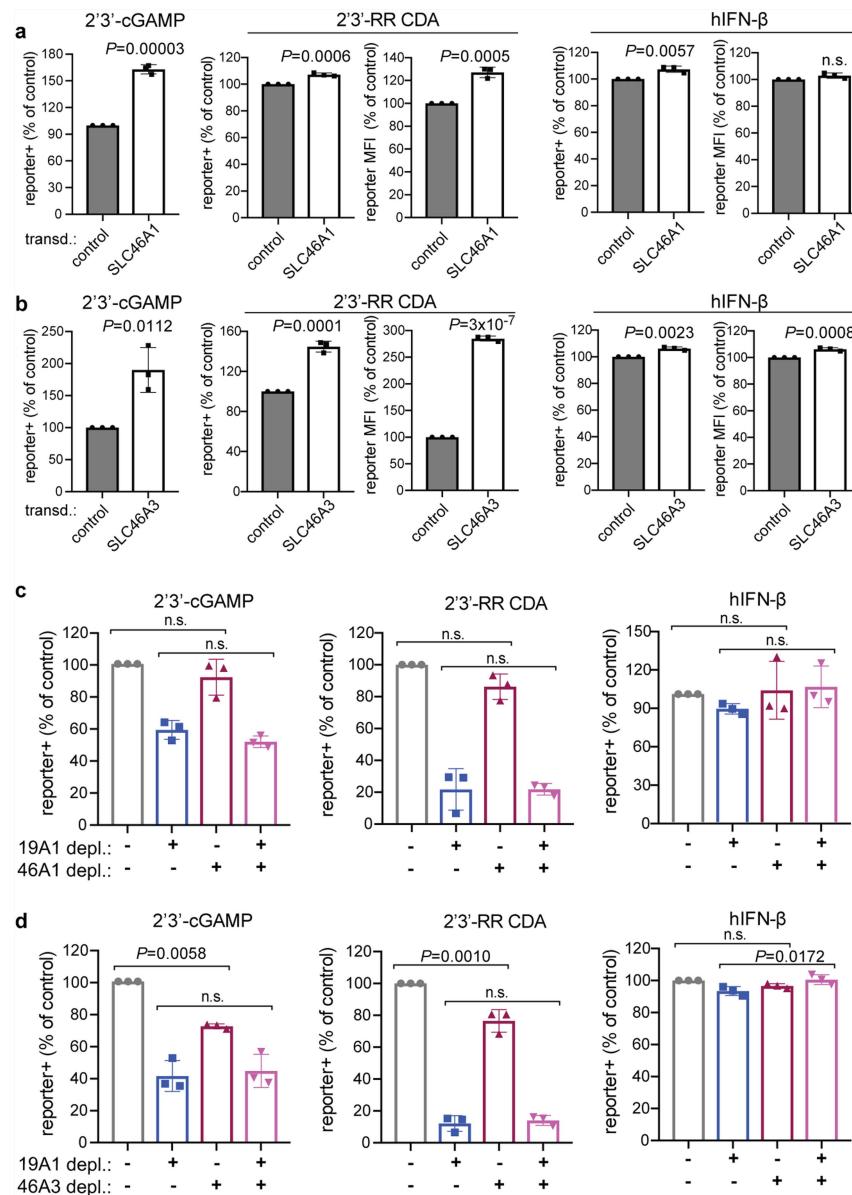


Extended Data Fig. 8 | 2'3'-cGAMP binds to SLC19A1. **a**, Left, SDS-PAGE analysis followed by Coomassie blue staining of His-tagged human SLC19A1 (purified on Ni-NTA) pull-downs with Sepharose beads coupled with 2'3'-cGAMP (+) or control Sepharose beads (-). Input is shown on the right. **b**, Western blots of the samples in **a** with SLC19A1 antibody. **c**, Pull-downs of SLC19A1 competed with CDNs. His-tagged SLC19A1 was incubated with no CDN or with the indicated competing CDNs

(250 μ M) before pull-downs with 2'3'-cGAMP-Sepharose, followed by SDS-PAGE and western blotting with SLC19A1 antibody. A pull-down with control Sepharose is shown for comparison. For gel source data, see Supplementary Fig. 1. **d**, SDS-PAGE analysis followed by Coomassie blue staining of pull-downs of mSTING CTD with 2'3'-cGAMP (+) or control (-) Sepharose. In all panels, data are representative of two independent experiments with similar results.



Extended Data Fig. 9 | RNA sequencing data of *STING* and *SLC19A1* mRNA expression in 934 human cancer cell lines available at the Cancer Cell Line Encyclopedia website. Expression is presented as transcripts per kilobase million (TPM). Data are downloaded from the European Bioinformatics Institute Gene expression Atlas (<https://www.ebi.ac.uk/gxa/home>). The dataset included three of the cell lines we examined, as shown.



Extended Data Fig. 10 | The effect of *SLC46A1* and *SLC46A3* expression on CDN-induced reporter activation. **a, b**, Enforced expression of *SLC46A1* and *SLC46A3* affects the responses of THP-1 cells to CDNs. Control THP-1 cells (transduced with empty expression vector) or *SLC46A1*-transduced THP-1 cells (**a**), or control THP-1 cells or *SLC46A3*-transduced cells (**b**) were stimulated with 2'3'-RR CDA ($1.25 \mu\text{g ml}^{-1}$), 2'3'-cGAMP ($15 \mu\text{g ml}^{-1}$) or IFN- β (100 ng ml^{-1}). tdTomato reporter expression was measured by flow cytometry 18–22 h after stimulation. **c, d**, *SLC46A1* or *SLC46A3* depletions had little or no effects on cellular responses to CDNs, and combining depletion of *SLC46A1* or *SLC46A3* with *SLC19A1* depletion had no additional effect compared to *SLC19A1*

depletion alone. THP-1 cells were transduced with non-targeting control CRISPRi gRNAs or *SLC19A1*-targeting CRISPRi gRNA in combination with a second control CRISPRi gRNA or *SLC46A1*-targeting CRISPRi gRNA in (**c**) or *SLC46A3*-targeting gRNA in (**d**). Cells were stimulated with 2'3'-RR CDA ($1.67 \mu\text{g ml}^{-1}$), 2'3'-cGAMP ($10 \mu\text{g ml}^{-1}$) or IFN- β (100 ng ml^{-1}). tdTomato reporter expression was measured by flow cytometry 18–22 h after stimulation. Combined data of three independent experiments. Statistical analysis was performed using unpaired two-tailed Student's *t*-tests (**a, b**) or one-way ANOVA followed by post hoc Tukey's test when comparing only the effects of depleting *SLC46A1* (**c**) or *SLC46A3* (**d**). Data are mean \pm s.e.m. of $n = 3$ independent replicates.

Reporting Summary

Nature Research wishes to improve the reproducibility of the work that we publish. This form provides structure for consistency and transparency in reporting. For further information on Nature Research policies, see [Authors & Referees](#) and the [Editorial Policy Checklist](#).

Statistical parameters

When statistical analyses are reported, confirm that the following items are present in the relevant location (e.g. figure legend, table legend, main text, or Methods section).

n/a Confirmed

- The exact sample size (n) for each experimental group/condition, given as a discrete number and unit of measurement
- An indication of whether measurements were taken from distinct samples or whether the same sample was measured repeatedly
- The statistical test(s) used AND whether they are one- or two-sided
Only common tests should be described solely by name; describe more complex techniques in the Methods section.
- A description of all covariates tested
- A description of any assumptions or corrections, such as tests of normality and adjustment for multiple comparisons
- A full description of the statistics including central tendency (e.g. means) or other basic estimates (e.g. regression coefficient) AND variation (e.g. standard deviation) or associated estimates of uncertainty (e.g. confidence intervals)
- For null hypothesis testing, the test statistic (e.g. F , t , r) with confidence intervals, effect sizes, degrees of freedom and P value noted
Give P values as exact values whenever suitable.
- For Bayesian analysis, information on the choice of priors and Markov chain Monte Carlo settings
- For hierarchical and complex designs, identification of the appropriate level for tests and full reporting of outcomes
- Estimates of effect sizes (e.g. Cohen's d , Pearson's r), indicating how they were calculated
- Clearly defined error bars
State explicitly what error bars represent (e.g. SD, SE, CI)

Our web collection on [statistics for biologists](#) may be useful.

Software and code

Policy information about [availability of computer code](#)

Data collection

Sequencing data was collected as part of the primary run processing using the innate HiSeq2500 and 4000 control software. Multiplexed sequencing data were demultiplexed using the BCL2Fastq program (version 2.17 and later). Flow cytometers: BD LSR Fortessa, BD LSR Fortessa X20 and BD LSR II. Flow data collection: BD FACSDiva version 6.1.3. RT-qPCR: Bio-Rad C1000 Thermal Cycler; beta counter: LS6500 Liquid Scintillation Counter (Beckman Coulter); Western blot infrared imager: Odyssey CLx System (LI-COR)

Data analysis

the Python-based ScreenProcessing pipeline (<https://github.com/mhorlbeck/ScreenProcessing>) and MaGeCK version 0.5.2 were used to analyze the CRISPRi sequencing results. For all other statistical analyses, Prism Graphpad 8 was used. Flow data analyses: FlowJo version 10.5.3; RT-qPCR: Bio-Rad CFX Manager 3.1

For manuscripts utilizing custom algorithms or software that are central to the research but not yet described in published literature, software must be made available to editors/reviewers upon request. We strongly encourage code deposition in a community repository (e.g. GitHub). See the Nature Research [guidelines for submitting code & software](#) for further information.

Data

Policy information about [availability of data](#)

All manuscripts must include a [data availability statement](#). This statement should provide the following information, where applicable:

- Accession codes, unique identifiers, or web links for publicly available datasets
- A list of figures that have associated raw data
- A description of any restrictions on data availability

Raw sequencing data from the CRISPRi screens are available at NCBI GEO (GEO accession number GSE134371)

Field-specific reporting

Please select the best fit for your research. If you are not sure, read the appropriate sections before making your selection.

Life sciences Behavioural & social sciences Ecological, evolutionary & environmental sciences

For a reference copy of the document with all sections, see [nature.com/authors/policies/ReportingSummary-flat.pdf](https://www.nature.com/authors/policies/ReportingSummary-flat.pdf)

Life sciences study design

All studies must disclose on these points even when the disclosure is negative.

Sample size	Preliminary experiments were the basis of power calculations, which were based on the magnitude of the preliminary effects and the desired level of statistical significance. The experiments were always repeated, usually multiple times, to ensure reproducibility
Data exclusions	no data were excluded from the analysis
Replication	the experiments were independently repeated multiple times, and statistical tests have been performed to ensure reproducibility. Information on statistical tests and reproducibility are described in the figure legends.
Randomization	these studies did not involve the comparison of different animals or patients, therefore randomization was not necessary
Blinding	Blinding was not relevant as the reported data was not based on subjective observations, but quantitative measurements, including flow cytometry, radio-activity, fluorescence etc. Nonetheless, samples were allocated an arbitrary number during analyses.

Reporting for specific materials, systems and methods

Materials & experimental systems

n/a	Involved in the study
<input checked="" type="checkbox"/>	<input type="checkbox"/> Unique biological materials
<input type="checkbox"/>	<input checked="" type="checkbox"/> Antibodies
<input type="checkbox"/>	<input checked="" type="checkbox"/> Eukaryotic cell lines
<input checked="" type="checkbox"/>	<input type="checkbox"/> Palaeontology
<input type="checkbox"/>	<input checked="" type="checkbox"/> Animals and other organisms
<input type="checkbox"/>	<input checked="" type="checkbox"/> Human research participants

Methods

n/a	Involved in the study
<input checked="" type="checkbox"/>	<input type="checkbox"/> ChIP-seq
<input type="checkbox"/>	<input checked="" type="checkbox"/> Flow cytometry
<input checked="" type="checkbox"/>	<input type="checkbox"/> MRI-based neuroimaging

Antibodies

Antibodies used

antibody name; supplier name; clone name; catalogue number; lot number; dilution; vendor website

rabbit-anti-human TBK1 mAb; Cell Signaling Technologies; D1B4; #3504; 4; 1:500; <https://www.cellsignal.com/products/primary-antibodies/tbk1-nak-d1b4-rabbit-mab/3504>

rabbit-anti-human phospho-TBK1 mAb; Cell Signaling Technologies; D52C2; #5483; 8; 1:1000; <https://www.cellsignal.com/products/primary-antibodies/phospho-tbk1-nak-ser172-d52c2-xp-rabbit-mab/5483>

rabbit-anti-human STING mAb; Cell Signaling Technologies; D2P2F; #13647; 1; 1:2000; <https://www.cellsignal.com/products/primary-antibodies/sting-d2p2f-rabbit-mab/13647>

rabbit-anti-human phospho STING mAb; Cell Signaling Technologies; D7C3S; #19781; 1; 1:1000; <https://www.cellsignal.com/products/primary-antibodies/phospho-sting-ser366-d7c3s-rabbit-mab/19781>

rabbit-anti-human phospho-IRF3 mAb; Cell Signaling Technologies; 4D4G; #4947; 13; 1:1000; <https://www.cellsignal.com/products/primary-antibodies/phospho-irf-3-ser396-4d4g-rabbit-mab/4947>

mouse-anti- β -Actin mAb; Cell Signaling Technologies; 8H10D10; #3700; 15; 1:1000; <https://www.cellsignal.com/products/primary-antibodies/b-actin-8h10d10-mouse-mab/3700>

goat-anti-mouse IgG IRDye 680RD conjugated; LI-COR Biosciences; polyclonal; #926-68070; c80619-05; 1:5000; <https://www.licor.com/bio/reagents/irdye-680rd-goat-anti-mouse-igg-secondary-antibody>

donkey-anti-rabbit IgG IRDye 800CW conjugated; LI-COR Biosciences; polyclonal; #926-32213; c80125-15; 1:5000; <https://www.licor.com/bio/reagents/irdye-800cw-donkey-anti-rabbit-igg-secondary-antibody>

donkey-anti-rabbit IgG IRDye 680RD conjugated; LI-COR Biosciences; polyclonal; #926-68073; c80116-07; 1:5000; <https://www.licor.com/bio/reagents/irdye-800cw-donkey-anti-rabbit-igg-secondary-antibody>

rabbit-anti-human IRF3 mAb; Abcam; ab76409; #EP2419Y; GR96792-10; 1:2000; <https://www.abcam.com/irf3-antibody-ep2419y-ab76409.html>

mouse-anti-human transferrin receptor mAb; Thermo Fischer Scientific; H68.4; #13-6800; RB232679; 1:1000; <https://www.thermofisher.com/antibody/product/Transferrin-Receptor-Antibody-clone-H68-4-Monoclonal/13-6800>

rabbit-anti-human SLC19A1 pAb; BosterBio; polyclonal; #PB9504; 0951512Da210465; 0.4 g/ml; <https://www.bosterbio.com/anti-slc19a1-picoband-trade-antibody-pb9504-boster.html>

APC-conjugated mouse-anti-human CD55 mAb; BioLegend; JS11; #311311; B183365; 1:50; <https://www.biolegend.com/en-us/products/apc-anti-human-cd55-antibody-1792>

mouse-anti-human CD59 mAb; BioLegend; p282; #304702; B204936; 1:250; <https://www.biolegend.com/en-us/products/purified-anti-human-cd59-antibody-890>

APC-conjugated goat-anti-mouse IgG; BioLegend; Poly4053; #405308; B158101; 1:100; <https://www.biolegend.com/en-us/products/apc-goat-anti-mouse-igg-minimal-x-reactivity-1383>

Validation

All antibodies used in flow cytometry and western blot were bought from commercial vendors and were validated by the manufacturers or relevant literature was cited on their websites (see vendor websites listed above)

Eukaryotic cell lines

Policy information about [cell lines](#)

Cell line source(s)

THP-1, K562, 293T cells, and RAW macrophages were present in the lab at the time this study began. MDA-MBA-453 cells were obtained from the Berkeley Cell Culture Facility. C1R cells were a generous gift from Veronika Spies (Fred Hutchinson Cancer Center, Seattle WA). 293T+hSTING cells were generated at Aduro Biotech Inc. L1210 cells were obtained from ATCC. 293F cells were a generous gift from David Veessler (University of Washington, Seattle WA)

Authentication

L1210 cells were authenticated by ATCC. MDA-MBA-453 were authenticated by the Berkeley Cell Culture Facility using karyotyping and/or PCR, other cell lines were not authenticated

Mycoplasma contamination

all cell lines were negative for mycoplasma contamination

Commonly misidentified lines (See [ICLAC](#) register)

No commonly misidentified cell lines were used

Animals and other organisms

Policy information about [studies involving animals](#); [ARRIVE guidelines](#) recommended for reporting animal research

Laboratory animals

Male and female C57BL/6J mice were obtained from The Jackson Laboratory (aged 4 to 20 weeks)

Wild animals

No wild animals were used

Field-collected samples

No field-collected samples were used

Human research participants

Policy information about [studies involving human research participants](#)

Population characteristics

We obtained peripheral blood lymphocytes from unidentified and randomly chosen healthy patients.

Recruitment

The patients were donors.

Flow Cytometry

Plots

Confirm that:

- The axis labels state the marker and fluorochrome used (e.g. CD4-FITC).
- The axis scales are clearly visible. Include numbers along axes only for bottom left plot of group (a 'group' is an analysis of identical markers).
- All plots are contour plots with outliers or pseudocolor plots.
- A numerical value for number of cells or percentage (with statistics) is provided.

Methodology

Sample preparation

Cells were harvested, washed and measured / sorted in RPMI or DMEM media

Instrument

Multicolor flow cytometry was performed on one of the following machines: LSR II, or LSR Fortessa or LSR X20 (BD)

Software

Data was analyzed using FlowJo 10.0

Cell population abundance

purity was greater than 95% after post sort analysis by flow cytometry

Gating strategy

Representative gating strategy for flow cytometry based sorting of the CRISPRi library of reporter-expressing THP-1 cells stimulated with CDNs. Cells were gated based on their forward scatter (FSC) and side scatter (SSC) using gate P1. P1-population was selected based on the expression of blue fluorescent protein (BFP, fluorescent marker for the CRISPRi gRNAs) and GFP (marker for the expression of the reporter construct) using gate P2. In gate P3, the doublet cells present in gate P2 were excluded. In gate P4, population P3 was gated based on tdTomato expression (see supplemental figure S2)

- Tick this box to confirm that a figure exemplifying the gating strategy is provided in the Supplementary Information.